# Thigmostimulation Alters Anatomical and Biomechanical Properties of Bioenergy Sorghum Stems

Omid Zargar, Qing Li, Chiedu Nwaobi, Matt Pharr, Scott A. Finlayson, and Anastasia Muliana

#### **Abstract**

Bioenergy sorghum [Sorghum bicolor (L.) Moench] is a tropical grass that can be used as a bioenergy crop but commonly suffers from stem structural failure (lodging) when exposed to mechanical stimuli, such as rain and wind. Mechanical stimulation can trigger adaptive growth in plant stems (thigmomorphogenesis) by activating regulatory networks of hormones, proteins, transcription factors, and targeted genes, which ultimately alters their physiology, morphology, and biomechanical properties. The goals of this study are 1) to investigate differences in the morpho-anatomical-biomechanical properties of internodes from control and mechanically-stimulated plants and 2) to examine whether the changes also depend on the plant developmental stages at the time of stimulation. The sweet sorghum cultivar Della was grown in a greenhouse under two growth conditions: with and without mechanical stimulation. The mechanical stimulation involved periodic bending of the stems in one direction during a seven-week growth period. At maturity, the anatomical traits of the stimulated and non-stimulated stems were characterized, including internode lengths and diameters, and biomechanical properties, including elastic (instantaneous) modulus, flexural stiffness, strength, and time-dependent compliance under bending. The morpho-anatomical and biomechanical characteristics of two internodes of the stems that were at different stages of development at the time of mechanical stimulation were examined. Younger internodes were more responsive and experienced more pronounced changes in length due to the stimulation when compared to the older internodes. Statistical analyses showed differences between the stimulated and non-stimulated stems in terms of both their anatomical and biomechanical properties. Mechanical stimulation produced shorter internodes with slightly larger diameters, as well as softer (more compliant) and stronger stems.

**Keywords:** Sorghum; Stems; Lodging; Mechanical stimulation; Morpho-anatomical properties; Biomechanical properties.

#### 1. Introduction

Sorghum is widely harvested for food, biofuel, and feedstock. However, sorghum plants are susceptible to structural failure (lodging) of both their stem and roots, which reduces yield. Root lodging is attributed to the weak bonding between the root and soil. Stem lodging is inherently a material and structural failure that commonly arises from wind-induced drag forces and is strongly correlated with stem mechanical properties [1-4]. Studies on the biomechanical properties of stems of grass plants, such as rice, sorghum, and maize, have focused on characterizing their elastic modulus, bending rigidity, and strength [3-5]. By examining the biomechanical properties of stems, breeders can classify and identify lodging-resistant and lodging-susceptible variants [6].

The morphological and anatomical traits and constituents of plants are the product of both genetic and environmental factors (responses to mechanical loading, temperature, soil conditions, etc.). For instance, repeated mechanical stimulation during growth (thigmostimulation), due to wind, rain, touch, etc., affects the growth and development of many plants [7]. The extent of the response depends not only on the species but also on the physiological stage of the plant during stimulation [8]. Boyer showed that by gently rubbing *Bryonia dioica* at either the upper or lower internodes, growth was reduced to less than 58% of the control plants (those without stimulation) [9]. Similarly, Meng et al. [10] concluded that tethering a 10-m lodgepole pine reduced the bending moment by 38%, which increased the elongation growth rate and decreased the secondary diameter growth, as compared to control trees. In another study, a gentle rubbing of the stem was found to slow the elongation of many plants, e.g., *Hordeum vulgate, Bryonia dioica, Cucumis sativus, Phaseolus vulgaris, Mimosa pudica*, and *Ricinus communis* [11]. In herbaceous and woody plants, mechanical stimulation typically increases stem diameter and decreases height [11-17].

Many studies on thigmostimulation have focused on the morpho-anatomical features of plants, while relatively few studies have addressed how mechanical stimulation affects the biomechanical properties of plant stems [14-16, 18]. Changes in stem physical properties (e.g., stiffness, viscosity, etc.) due to mechanical stimulation have been correlated with changes in their microstructural morphologies, e.g., rind thickness, number of vascular bundles in the pith, and the size, shape, and composition of cell walls [13-17]. Periodic mechanical stimulation from 7-14 weeks after planting increased the bending strength of sorghum stems by 12-71% depending on the genotype and internode position, while changes in the elastic modulus varied for different genotypes [16]. Bruchert and Gardiner [19] found that Sitka spruce (*Picea sitchensis*) exposed to wind had higher flexibility of the crown with higher flexural stiffness of the stem base compared to the wind-sheltered controls, which ultimately resulted in shorter trees with larger diameters and an overall lower modulus of elasticity. Likewise, Badel et al. [20] and Telewski [21] found that thigmostimulation of *Abies fraseri* decreased the elastic modulus of wood materials.

Changes in the plant's biomechanical properties can be attributed to cell wall components. Several studies have suggested that touch-induced morphogenic changes are associated with increases in the production of strengthening tissue, e.g., secondary cell walls with high lignin content, thus improving resistance to damage by lateral forces such as from wind [13, 22, 23]. Badel et al. [20] reported that the mechanical properties of cell walls depend on the cell wall structure, e.g., the microfibril angle (MFA), as well as on chemical composition, e.g., lignin, cellulose, and hemicellulose. Recently, Wu et al. [24] have shown that touch increased the cell wall stiffness and decreased cell elongation of Arabidopsis seedling hypocotyls, which was attributed to pectin degradation elicited by touch activation of ethylene signaling. Mechanical stimulation of *Brachypodium distachyon* elevated lignin, increased pectin methylesterase activity, and reduced release of carbohydrates from the cell wall [25]. These anatomical and microstructural changes also increased the rigidity of the stems.

Gomez et al. [26] implemented a three-point bending test for freshly harvested sorghum stems and found that stems with lower flexural stiffness and higher strength were correlated with lodging-resistance. Most studies have considered plant stems as elastic materials, but sorghum stems are known to exhibit pronounced viscoelastic responses [27], which will affect their response to wind loading at various speeds and frequencies. Limited information exists regarding the biomechanical properties of sorghum altered by mechanical stimulation. Lemloh et al. [16] characterized bending strength and tissue distributions (rind thickness, pith area, and vascular bundles) of sorghum internodes from stimulated and control plants grown in a growth chamber. Further investigation of other mechanical properties and anatomical and morphological features of plant stems modified by mechanical stimulation is needed to enhance our understanding on the thigmostimulation effect on plant biomechanics. Furthermore, it is not understood how mechanical stimulation influences the sorghum stems at various developmental stages and thereby impacts the biomechanical and anatomical properties of sorghum internodes.

This study explored the influence of periodic mechanical stimulation on the biomechanical properties and morpho-anatomical traits of internodes at different stages of development in bioenergy sorghum. The overall focus of this study was to provide insight into how mechanical stimulation alters biomechanical properties of sorghum stems with the goal of enhancing our understanding of the role of biomechanics in producing lodging-resistant plants. We hypothesized that mechanical stimulation would result in more pronounced changes in the biomechanical properties of elongating internodes (a younger internode at the time of stimulation) in bioenergy sorghum, e.g., elastic modulus, bending strength, flexural stiffness, and time-dependent compliance, as well as in more pronounced changes in anatomical traits, e.g., internode length and diameter and the morphological features of the rind and pith tissues.

#### 2. Materials and Methods

#### 2.1. Plant material

The sorghum cultivar Della was used for this research. Della is sweet sorghum that is suitable for use as a bioenergy feedstock. Growth of plants began on May 29th, 2020, in a greenhouse at Texas A&M University located at 30.6° N. The temperature was 26-30°C day/21-26°C night, and the photoperiod was 14 h day/10 h night, with supplemental light provided by high-pressure sodium lamps [27]. Plants were grown in pairs in 14.88 L pots (10 7/8 "Dia x 11 1/8" H) containing a fine sandy loam soil amended with 12.5% potting mix (Jolly Gardener C/20), and adequate water and nutrients (Osmocote 13-13-13 and soluble micronutrients) were provided. At 39 days after planting, half of the plants were mechanically stimulated, and the other half were not (control). Plants were harvested for mechanical testing at grain maturity 13 weeks after planting. Internodes were counted from the base of the plant upwards. The study focused on the response of internodes at different stages of development to mechanical stimulation, including internode 4 (older, around 7 cm, near the end of the elongation phase at the onset of stimulation) and internode 7 (younger, less than 1 cm, early in the elongation phase at the onset of stimulation).

# 2.2. Mechanical stimulation

An experimental apparatus ( $\sim$ 6 x 14 feet, see **Figure 1** and the sketch-up of the system in **Figure** S.1 in the Supplemental Document) capable of mechanically stimulating ~100 plants during growth in a greenhouse was constructed. The set-up consisted of a programmable controller/motor and linear actuator. The height of the frame was adjustable in accordance with the height of plants during their growth. The frame was integrated with round 3 mm diameter PVC rods placed parallel to the shorter side of the rectangular frame. The rods came into contact with the plants when the frame moved laterally, thereby inducing bending of the stems. At the beginning of stimulation, the average distance between the bottom of the stem (soil surface) and the rods was set to 43 cm. For most plants, when the stimulation started, the youngest internode was internode 7, which was less than 1 cm, and the total height from the 1st internode to the 7<sup>th</sup> internode was less than 40 cm at that point in time. When plants started to flower (around 8 weeks after planting), the rods were moved to a height of ~54 cm from the soil surface. The height of the structure was adjusted to ensure that plant stimulation did not cause failure at the internodes, as the top internodes were more flexible than the bottom internodes when the plants grew taller. The mechanical stimulation was applied periodically to induce cyclic bending in one bending axis at a frequency of 3 cycles per minute with a 20 cm amplitude continuously for two hours, followed by a six-hour resting period (see Figures 1a, b), before continuing the next stimulation cycle. These conditions were implemented to avoid any potential inertial effects in deforming the stems. Likewise, the relatively slow stimulation reduced the likelihood of damaging the stems during stimulation. Stimulation was performed continuously from 39 days after

planting to 13 weeks after planting. Non-stimulated (control) plants were grown on an adjacent bench under the same conditions in the same greenhouse.

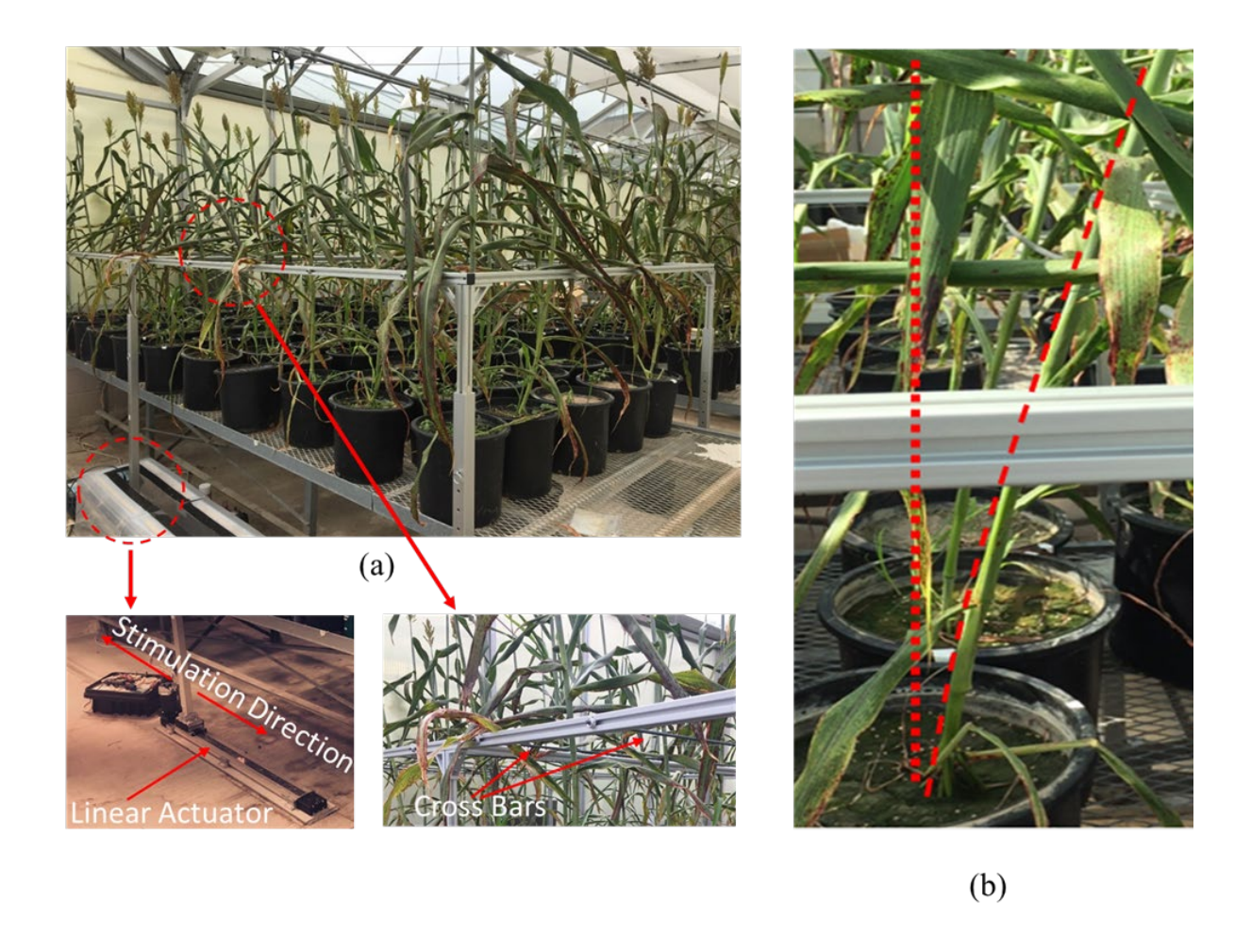


**Figure 1**: (a) Assembled apparatus for mechanical stimulation of plants in the greenhouse. (b) Lateral bending of stems during mechanical stimulation. In the photographs, the plants are at the flowering stage, which is approximately 2 months after planting.

# 2.3. Sample preparation for four-point bending tests

Plants were harvested 13 weeks after planting by cutting the stems at the soil level between 8 and 10 AM before greenhouse temperatures increased. Ten replicate plants were randomly sampled and the leaves were removed to avoid dehydration. Internodes 4 and 7 were selected for mechanical testing. These internodes were chosen to examine the influence of mechanical stimulation on the morpho-anatomical and biomechanical properties of stem tissues at different stages of development. All tests were conducted within

6 h after cutting the internodes. For bending experiments, samples were cut 25 mm past the nodes to produce a sufficiently long test specimen. Before the bending tests, the overall length and diameter of the specimens were measured using calipers. The diameter of the internodes was measured in 4 different positions to produce an averaged value.

#### 2.4. Sample preparation for morphological analysis

Stem cross-sections of stimulated and control plants were cut 4 weeks after anthesis in the middle of the 4th and 7th internodes with a small table saw and fixed overnight in FAA solution (50% ethanol, 5% acetic acid, and 4% formaldehyde). The samples were then paraffin-embedded, sectioned to 20 microns, stained with FASGA solution [28], and scanned at 20X using brightfield optics, which was performed in the histology lab of the Texas A&M College of Veterinary Medicine & Biomedical Sciences.

# 2.5. Four-point bending tests

Bending tests were conducted on sorghum internodes (internodes 4 and 7) at room temperature using a four-point bending device fixed to an Instron 5943 with a 1 kN load cell at a displacement rate of 10 mm min<sup>-1</sup>. **Figure 2** shows images of a four-point bending test. The loading anvils (top) contacted the internode of interest, and the supports (bottom) were placed near the nodes. In all tests, the span lengths between the loading anvils were kept at 1/3 of the internode length (BSI, 2005; Structural round timber - Test methods) (**Figure 2**). We used rubber layers on the supports to decrease slippage issues between the supports and the internodes. Failure at the end of the bending tests was classified into two different general modes. In one case, failure arose from the breaking of the rind and subsequent separation from the pith along the length of the stem in the tension region (bottom surface) of the bending test (see **Fig. 3 a and d**). In the other case, cracks formed in the circumferential direction of the stem, in the compression region, and wrinkling of the rind was also observed; this failure is common in fiber composites because the circumferential direction is often weaker than the axial direction and a thin outer layer can easily buckle under compression (see **Fig. 3 b and c**). In both cases, water flowed out of the specimens after the initiation of failure (see **Fig. 3c and d**).

In the four-point bending tests of the stimulated plants, we implemented two testing scenarios to examine whether the direction of mechanical stimulation (compression vs. tension) impacted the internodes' overall biomechanical properties in a direction-dependent manner. In scenario one, the bending force was applied to induce bending in the same direction that the plant experienced from the mechanical stimulation during growth (i.e., the region that was under compression during the stimulation was also under compression during the four-point bending test, and likewise for the tension region). In scenario two, the bending force was applied to induce bending in the opposite direction of the mechanical stimulation

(i.e., the region that was under compression during the stimulation was under tension during the four-point bending test). Since directional differences were not observed, the data were combined to generally represent stimulated internodes.

Additionally, we conducted limited four-point bending creep tests from internodes 4 and 7 of stimulated and control plants to show the significant effect of viscoelastic responses of the stems. The discussion of the creep tests is given in the Supplemental Document. This preliminary creep tests should motivate future study to examine the viscoelastic responses of plant stems.

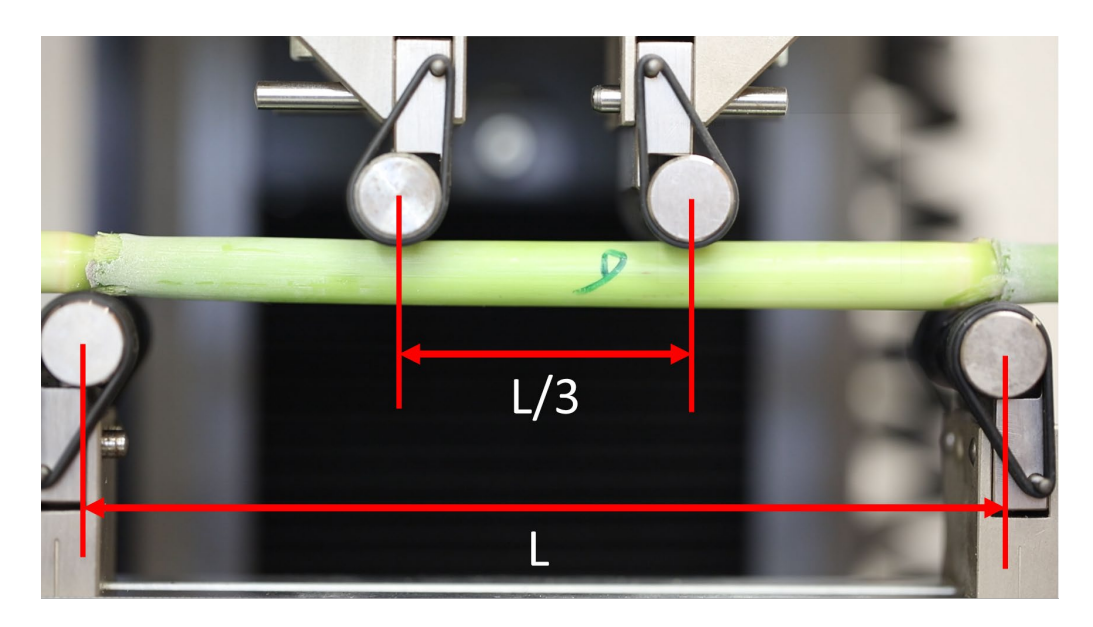
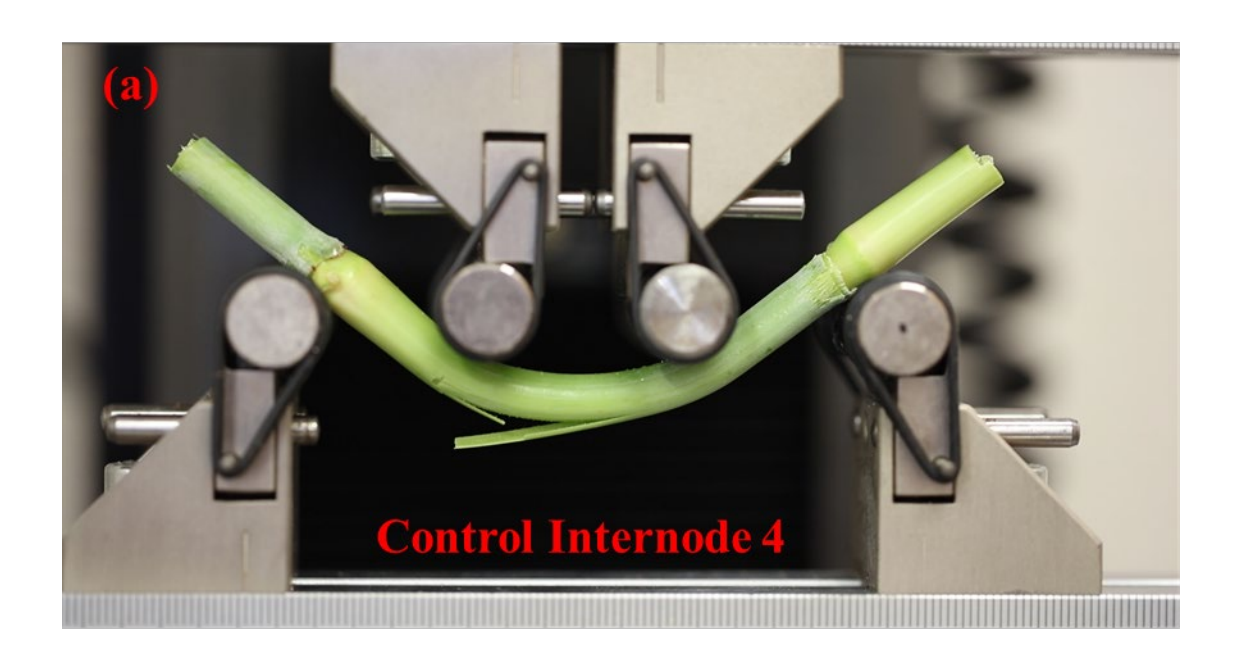
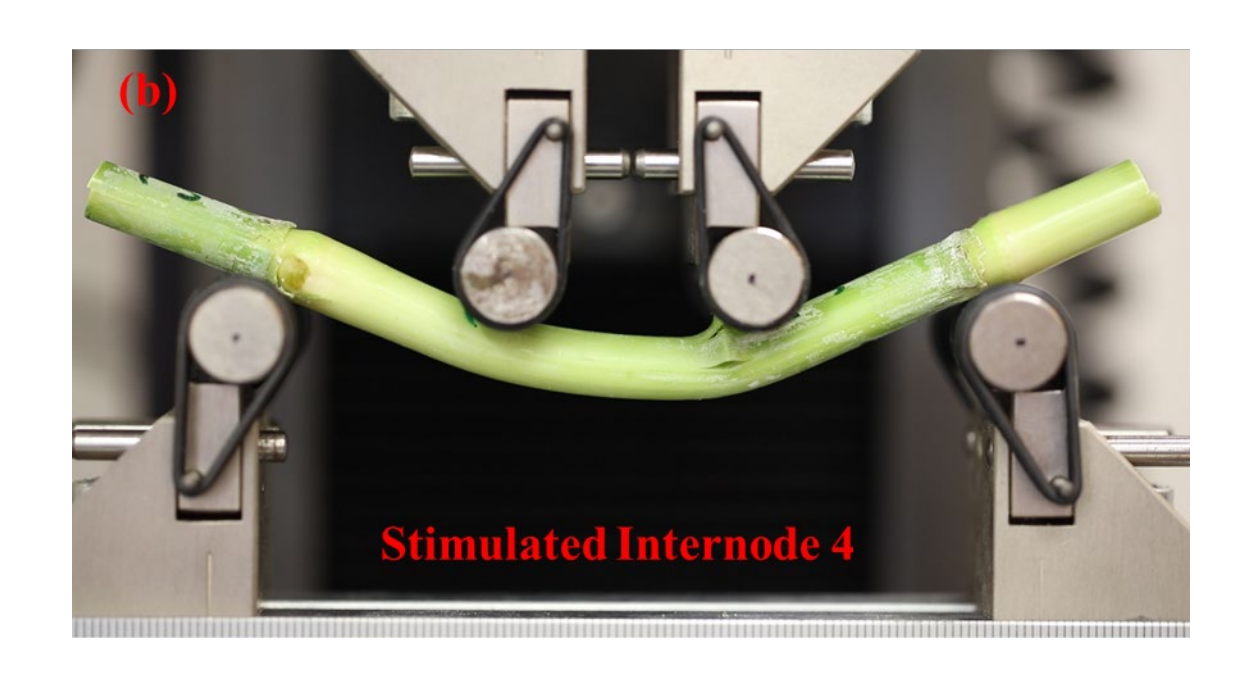
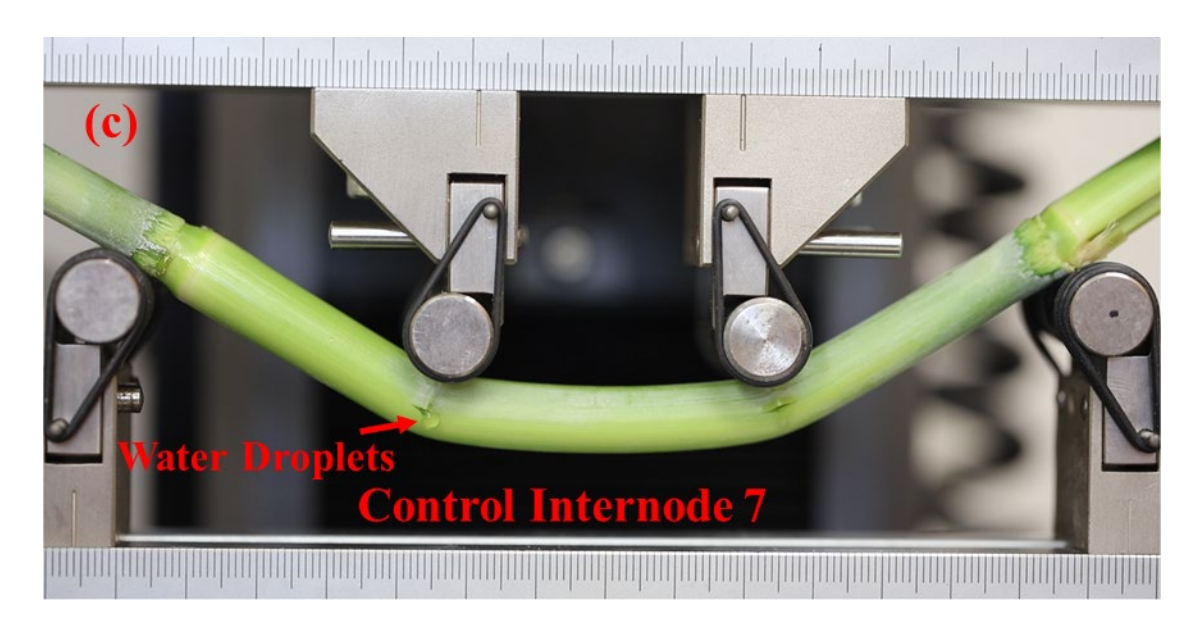
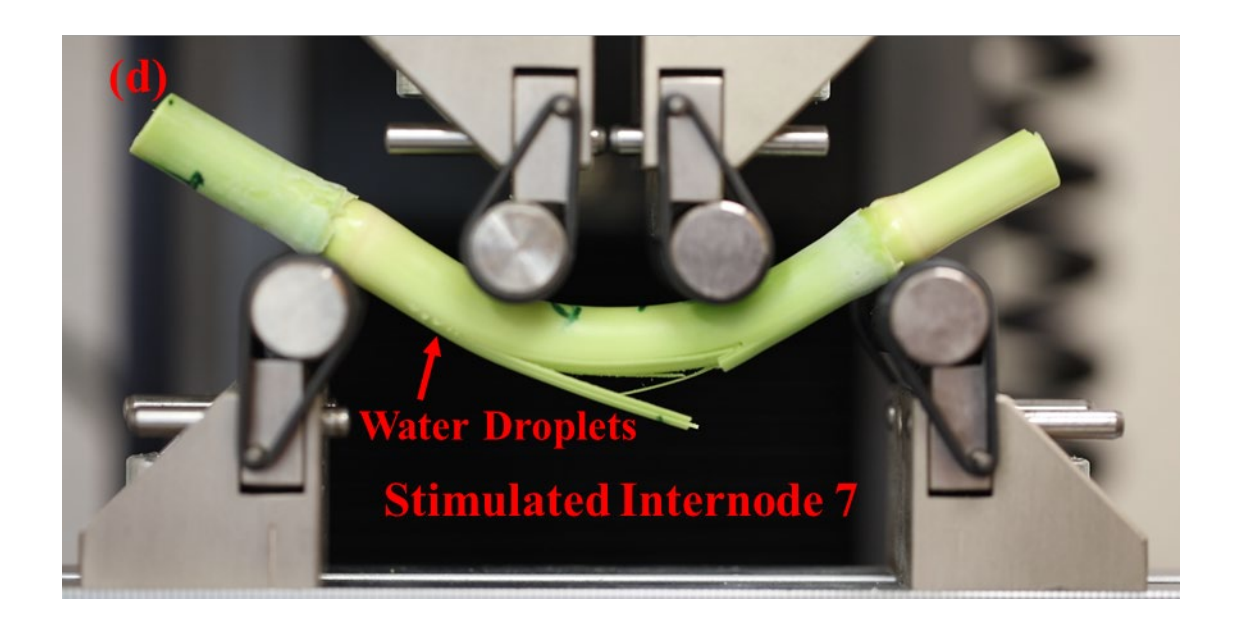


Figure 2: Four-point bending test geometry.









**Figure 3**: Mechanical failure of the control and stimulated plant stems: (a) control internode 4, (b) stimulated internode 4, (c) control internode 7, and (d) stimulated internode 7.

# 2.6. Modeling of the stem deformations under bending tests

From the observed experimental results, the stems undergo relatively large displacements prior to failure, which is attributed to large rotations, and the overall recorded force-displacement responses indicate nonlinear responses, as will be shown later. The bending responses depend on the geometrical parameters of the stems and the material responses to mechanical loading. A beam bending model was used to simulate the four-point bending tests and extract the biomechanical properties of the stems. Additionally, previous studies have indicated that plant tissues and especially fresh plant stems exhibit pronounced viscoelastic responses [27].

In this study, we considered the overall stem bending as exhibiting a nonlinear viscoelastic response and undergoing large deformations attributed to large rotations while the strains are relatively small. From available biomechanical studies [29, 30], plant tissues typically fail at relatively low strains, e.g., less than 10%; as such, modeling the tissues as being under relatively small strains is reasonable. We adopted a material model for the stems that was previously developed for polymers [31, 32]. We also used the Reissner beam theory, which incorporates large deformation bending with a relatively small strain [33]. An implementation of a nonlinear viscoelastic model to the Reissner beam theory can be found in [34]. A detailed discussion on the large deformation four-point bending analyses with the nonlinear viscoelastic material is given in the Supplemental Document.

The constitutive material model for the nonlinear viscoelastic stem is given as:

$$F(\varepsilon) = \sigma(0) J(t) + \int_{0}^{t} J(t-s) \frac{d \sigma(s)}{ds} ds$$
(1)

where the left-hand side  $F(\varepsilon)$  is the axial stress measure that depends on the axial strain  $\varepsilon(t)$ ;  $\sigma(t)$  is the axial stress; and J(t) is the normalized creep function, which is a non-dimensional time-dependent function with J(0)=1. In the absence of time-dependent effects,  $F(\varepsilon)=\sigma(0)$ . To incorporate the nonlinear elastic response of the stem tissue, with an assumption that tension and compression behaviors are the same, the following model for the axial stress measure is implemented:

$$F(\varepsilon) = \sigma = \frac{E_0}{\beta} \left( e^{\beta |\varepsilon|} - 1 \right) \frac{\varepsilon}{|\varepsilon|} \tag{2}$$

where  $E_0$  and  $\beta$  are material parameters that can be determined from experimental data. Linearization of Eq. (2) reduces to a linear elastic response, i.e.  $\sigma = E_0 \varepsilon$ , with  $E_0$  being the elastic modulus of the material. The material parameter  $\beta$  characterizes the nonlinear responses of the materials, which is correlated with the maximum stress (strength) of materials. To interpret the nonlinear response, we take a Taylor series expansion of Eq. (2) up to a second order and evaluate it at zero, i.e.,  $\sigma = E_0 \varepsilon + \frac{E_0 \beta}{2} \varepsilon^2$ . It is seen that increasing  $\beta$  increases the stress at a fixed strain, as will be shown later. A positive or negative value of  $\beta$  indicates a stiffening or softening response, respectively.

In analyzing bending deformations, the axial strain is given as  $\varepsilon(x,y,z) = -y \kappa(x,t)$ , where x is the longitudinal axis of the beam, y is the lateral location along the beam cross-section, and  $\kappa(x,t)$  is the beam curvature that varies in space and time. The internode is modeled as a beam with a circular cross-section of a radius r. Imposing the equilibrium equation  $M = -\int_A y \, \sigma dA$ , where M = M(x,t) is an internal bending moment, Eq. (1) can be rewritten as:

$$\int_{A_0} yF(\varepsilon) dA = \int_{A_0} y\sigma(0) J(t)dA + \int_{A_0} y \int_0^t J(t-s) \frac{d\sigma(s)}{ds} ds dA$$

$$\int_{-r}^r \frac{E_0}{\beta} \left( e^{\beta|y\kappa(x,t)|} - 1 \right) \operatorname{sgn}(\varepsilon) \left( 2\sqrt{r^2 - y^2} \right) dy = M(x,0) J(t) + \int_0^t J(t-s) \frac{dM(x,s)}{ds} ds$$
(3)

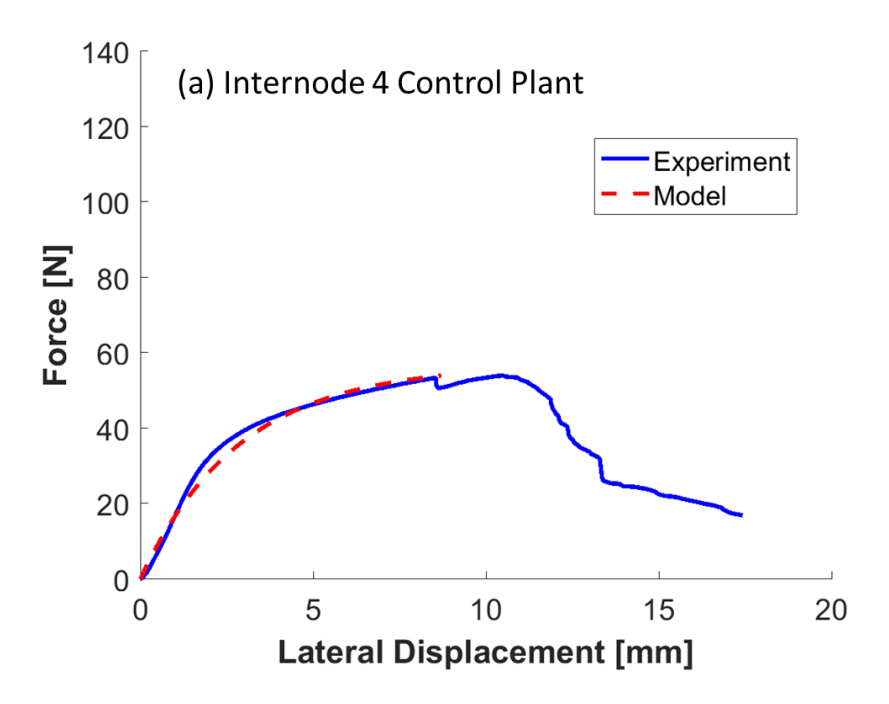
Eq. (3) defines the governing equation of beam bending with nonlinear viscoelastic response.

Finally, the lateral displacement of the beam under bending  $u_{\nu}(x,t)$  can be determined as follows:

$$\frac{du_{y}(x,t)}{dx} = \sin \varphi(x,t); \quad \frac{d\varphi(x,t)}{dx} = \kappa(x,t)$$
(4)

where  $\varphi(x,t)$  is the rotational angle. In simulating the four-point bending tests, the following boundary conditions are considered:  $M(0,t) = u_v(0,t) = \varphi(L/2,t) = 0$  where L/2 is the mid-span of the beam.

From the quasi-static four-point bending test, where the time-dependent part is insignificant due to a relatively fast loading rate, the elastic (instantaneous) modulus and strength of the stem tissue can be calibrated. **Figure 4** shows examples of force-displacement responses from the model and experiment, in which responses from the model were used to determine the mechanical properties of the stems. The strength was determined at the location of the first "sudden drop" in the force-displacement curves, i.e., around 8 mm in **Figure 4a** and 6 mm in **Figure 4b**, which corresponds to the onset of cracking in the stems. The elastic modulus and nonlinear parameter were calibrated to match the force-displacement response prior to the start of failure. Unpaired t-tests were used to assess the significance of differences between the calibrated parameters of the stimulated and control internodes. The unequal number of samples between treatments arose from plants that were removed from the data set due to significant sliding of the samples on the supports, axial rotation of the samples, and/or movement of the supports during testing, as well as plants that demonstrated stem lodging in the greenhouse. However, in calculating the elastic modulus, more samples could be used as valid tests, as only data from the early loading stage (e.g., before significant slipping was observed in some specimens) were required.



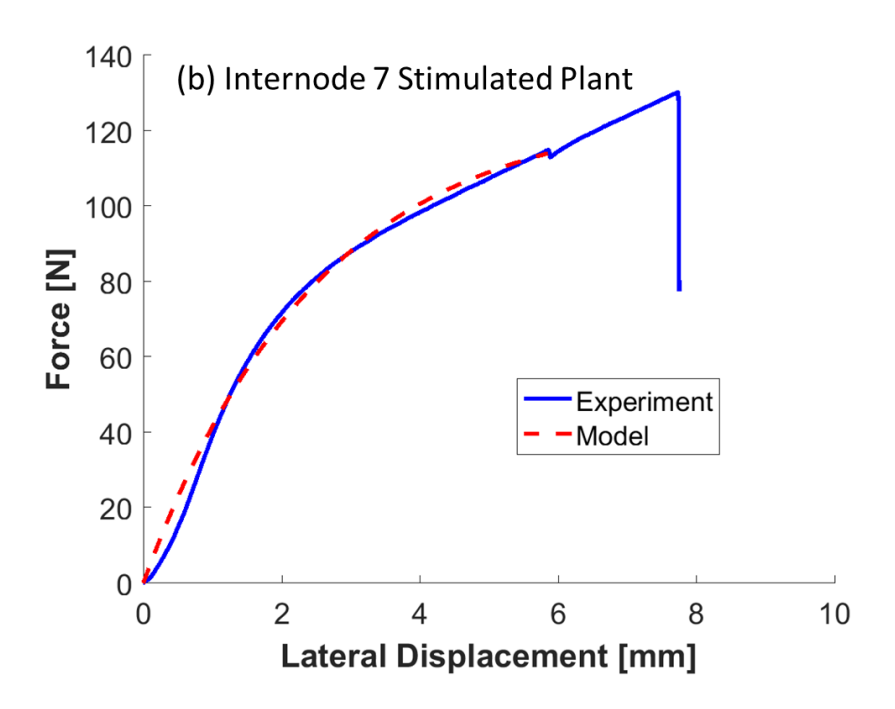


**Figure 4**: Experimental data and corresponding model of four-point bending tests to characterize material properties from: (a) internode 4 and (b) internode 7.

# 2.7. Data analysis

Force-displacement data were acquired through the Instron software (Bluehill® Universal 4.01) and processed in MATLAB® R2016b version 9.1. For force-displacement plots, each force represents the average of all the samples at a specified displacement. When a given plant reached its strength (maximum stress before failure starts, as defined in the previous section), it was removed from the averaging. For instance, if a plant reached its strength at a displacement of 8 mm, that specific plant was removed from the data set in determining the average force for displacements larger than 8 mm. Likewise, the last point in the plots represents the largest displacement among all the samples. Statistical analysis was conducted using R (version 4.1.1) and RStudio (version 1.4.1717). Data that did not follow a normal distribution were normalized. Two-way analysis of variance (ANOVA) followed by planned contrasts (where appropriate) and unbalanced t-tests were used to identify differences in anatomical traits and biomechanical properties between control and stimulated plants, with the significance level at  $p \le 0.05$ .

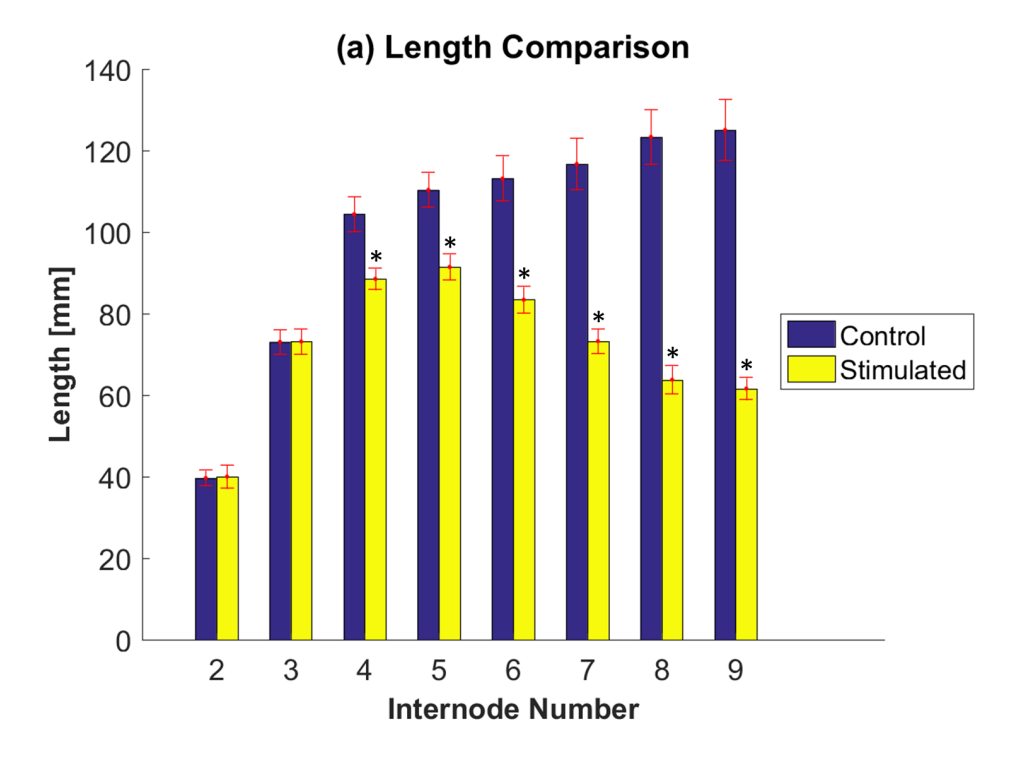
# 3. Results

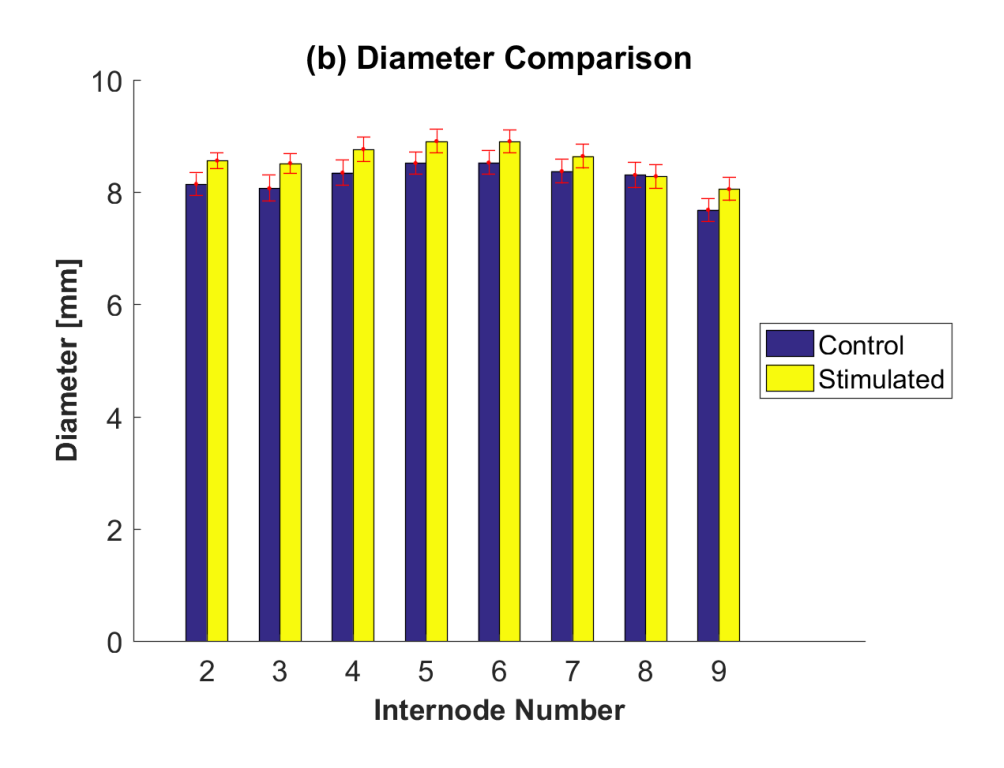
# 3.1. Comparison of anatomical traits between stimulated and non-stimulated plants

Anatomical traits, including the length and diameter of the internodes, are shown in **Figure 5**. The total height of stimulated plants was less than that of control plants, as can be seen in **Figure 6**. Mechanical stimulation decreased the lengths of all internodes, except for internodes 2 and 3 (statistical analyses shown in **Table S.2** in the Supplemental Document). From the two-way ANOVA analysis in **Table S.2** the total decrease in the lengths of internodes 8 and 9 was significantly greater than that in internodes 6 and 7, which in turn was significantly greater than that in internodes 4 and 5, indicating that internodes that were younger (internodes 6-9) when mechanical stimulation was initiated showed more pronounced changes in length compared to the internodes that were nearly fully elongated (internodes 4 and 5). When the diameter of each pair of internodes were compared independently, there was a slight increase in all stimulated internodes. From the two-way ANOVA result, mechanical stimulation also increased internode diameter, but this effect was not dependent on internode position (**Table S.3** in the Supplemental Document). When examining stems under bending, the important geometrical parameter is the second moment of area, i.e.

 $I = \frac{\pi d^4}{64}$ , where d is the diameter of the cross-section. Thus, slight changes in the diameter can have a pronounced effect on the bending responses of the stems. **Figure 5** shows the second moment of area, and the corresponding statistical analyses are given in **Table S.3** in the Supplemental Document. The second moment of area of stimulated plants was greater than that of controls, in agreement with the effects of

mechanical stimulation on internode diameter.





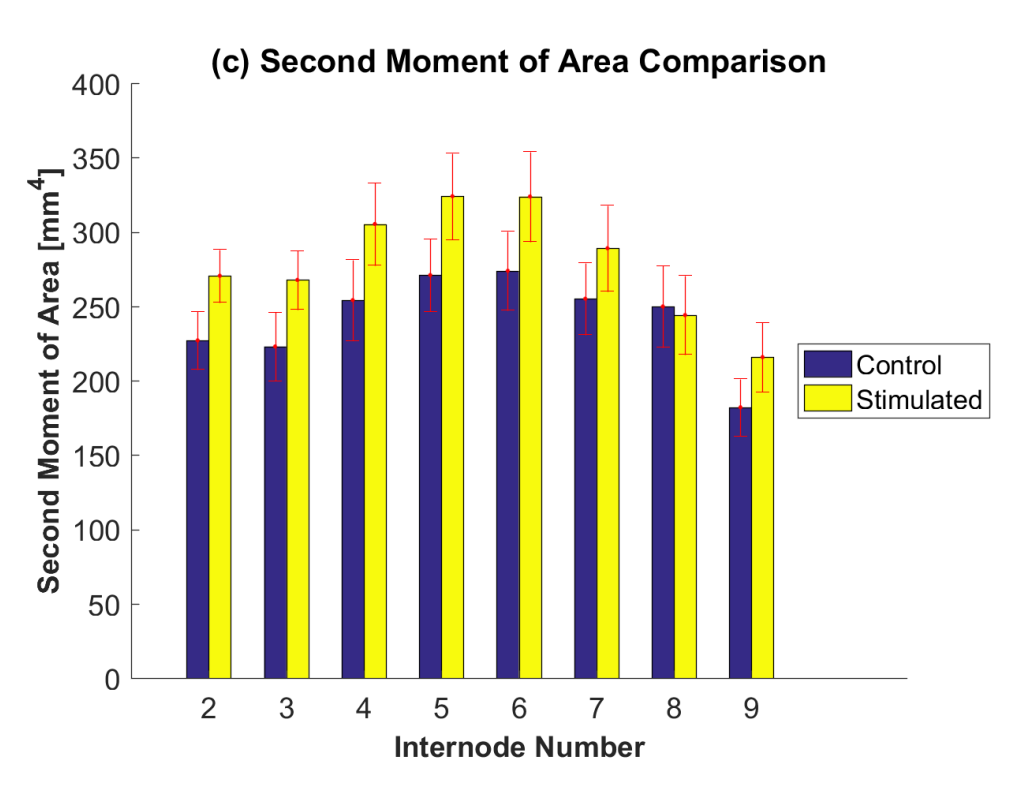
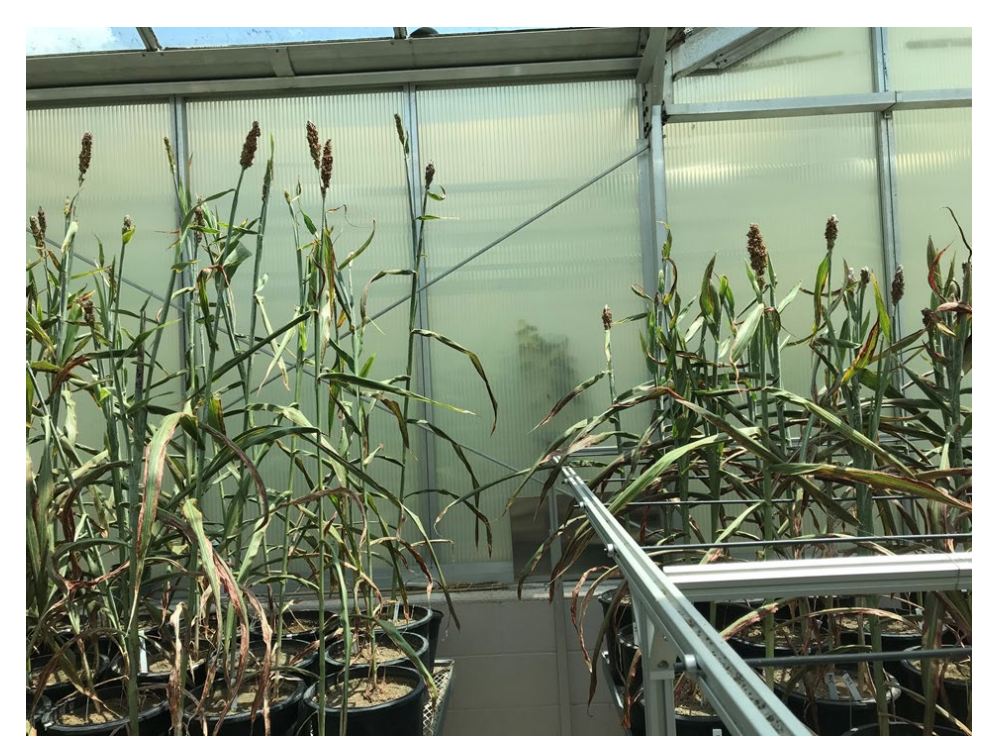


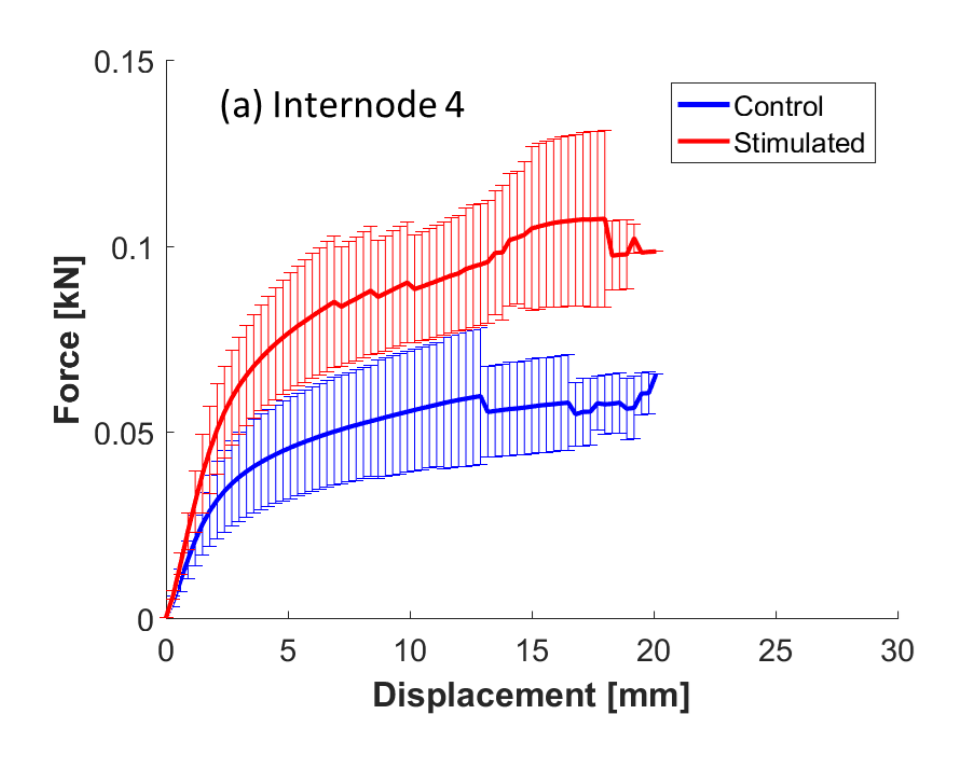
Figure 5: Comparisons of anatomical traits of the control and stimulated plants: (a) internode length, (b) diameter, and (c) second moment of area; data are means  $\pm$  SE (Standard Error) and Asterisks (\*) indicate a significant difference in internode length between control and stimulated plants at  $\alpha = 0.05$ .

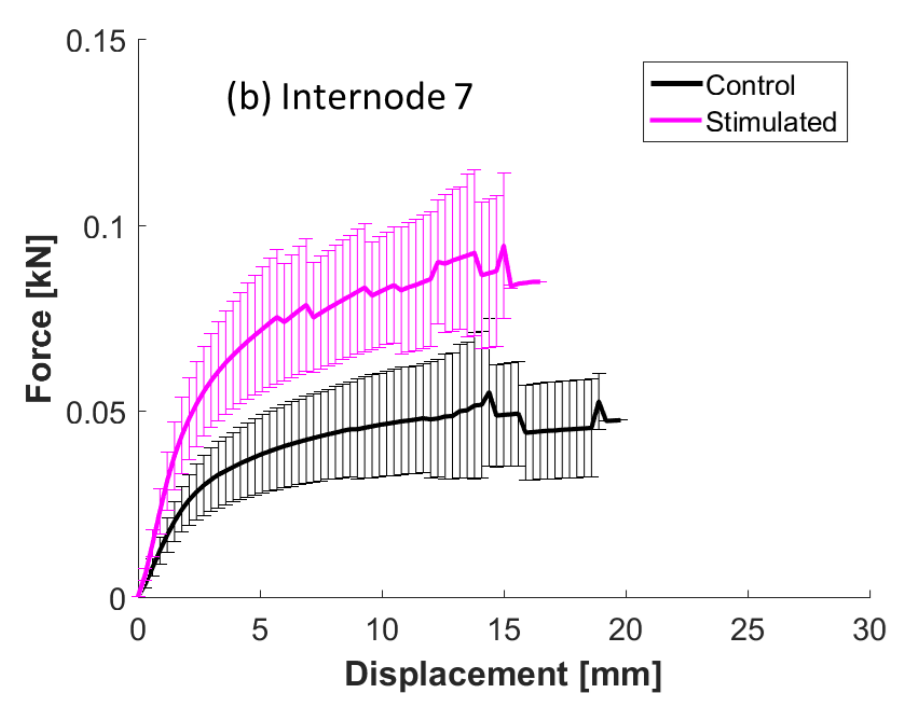


**Figure 6**: A comparison between control and stimulated plant in a group (the left group is control, and the right group is stimulated).

# 3.2. Comparison of mechanical properties between stimulated and non-stimulated plants

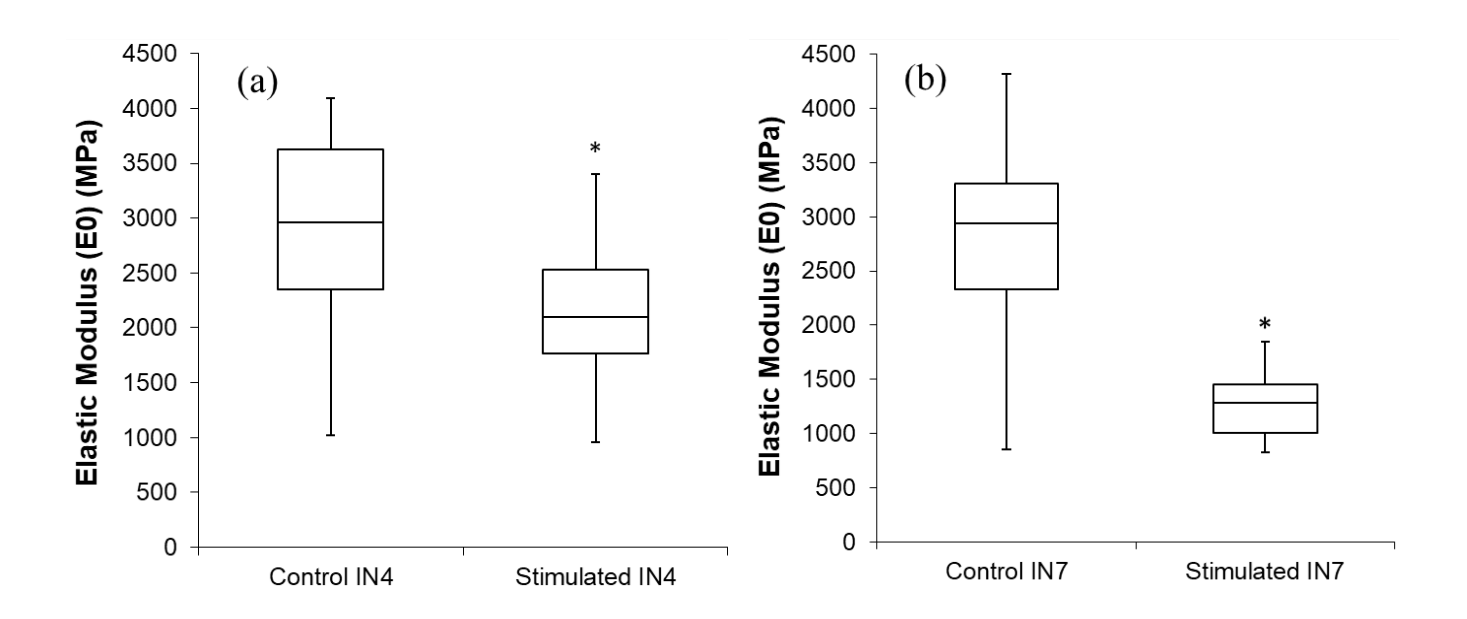
Figure 7 shows representative plots from quasi-static four-point bending tests of internodes 4 and 7 with the recorded bending force and lateral deformation at the location of the prescribed load. When the mechanical stimulation during growth was initiated, internode 4 was almost finished elongating while internode 7 was at an early stage of elongation. Clear differences were apparent in the responses of the stimulated and control plants, which are associated with changes in the morpho-anatomical and biomechanical properties of the plants, as will be discussed later. In both internodes 4 and 7, the stimulated stems supported much larger bending forces (about twice as much), which was attributed to changes in the stems' lengths, diameters, moduli, and strengths. The stems' elastic moduli and strength are discussed below and summarized in Figure 8.





**Figure 7**: Force and lateral displacement of sorghum stems during four-point bending of control and stimulated plants: (a) internode 4 and (b) internode 7; data are means  $\pm$  SD (Standard Deviation)

The calibrated biomechanical parameters, i.e., elastic modulus  $E_0$ , strength, flexural stiffness, and nonlinear parameter  $\beta$ , and the corresponding box plots are shown in **Figure 8.** In this study, the strength was defined as the axial stress immediately before the first "sudden drop" in the force-displacement curves (see Figure 4). The sudden drop indicates the start of failure/damage in the bending test. Overall, the stimulated plants showed significantly smaller values of elastic modulus (softer material behavior) but relatively greater strength in both internodes 4 and 7. Figure 8 indicated that significant differences existed between stimulated and control plants for both internode 4 and 7 in terms of elastic moduli (Fig. 8a, b) and strength (Fig. 8c, d). Overall, the mechanically stimulated plants were softer (more compliant) than the control group. When also accounting for differences in geometry (e.g., incorporating the effects of varying diameters produced through the different growth treatments), internode 7 of stimulated plants still exhibited less flexural stiffness (a product of elastic modulus and second moment of area of the cross-section) as compared to the control plants; this trend was the same for internode 4, although the flexural stiffness of stimulated internode 4 was not significantly different from control. Figure 8d shows that there was also a large difference between control and stimulated plants with respect to  $\beta$  (nonlinear material parameter) for internodes 4 and 7. The coefficient  $\beta$  is defined such that a larger value of  $\beta$  indicates a greater strength. The stimulated plants showed relatively larger (less negative)  $\beta$  values compared to control plants for both internodes 4 and 7. The statistical results are provided in **Table S.4** in the Supplemental Document.



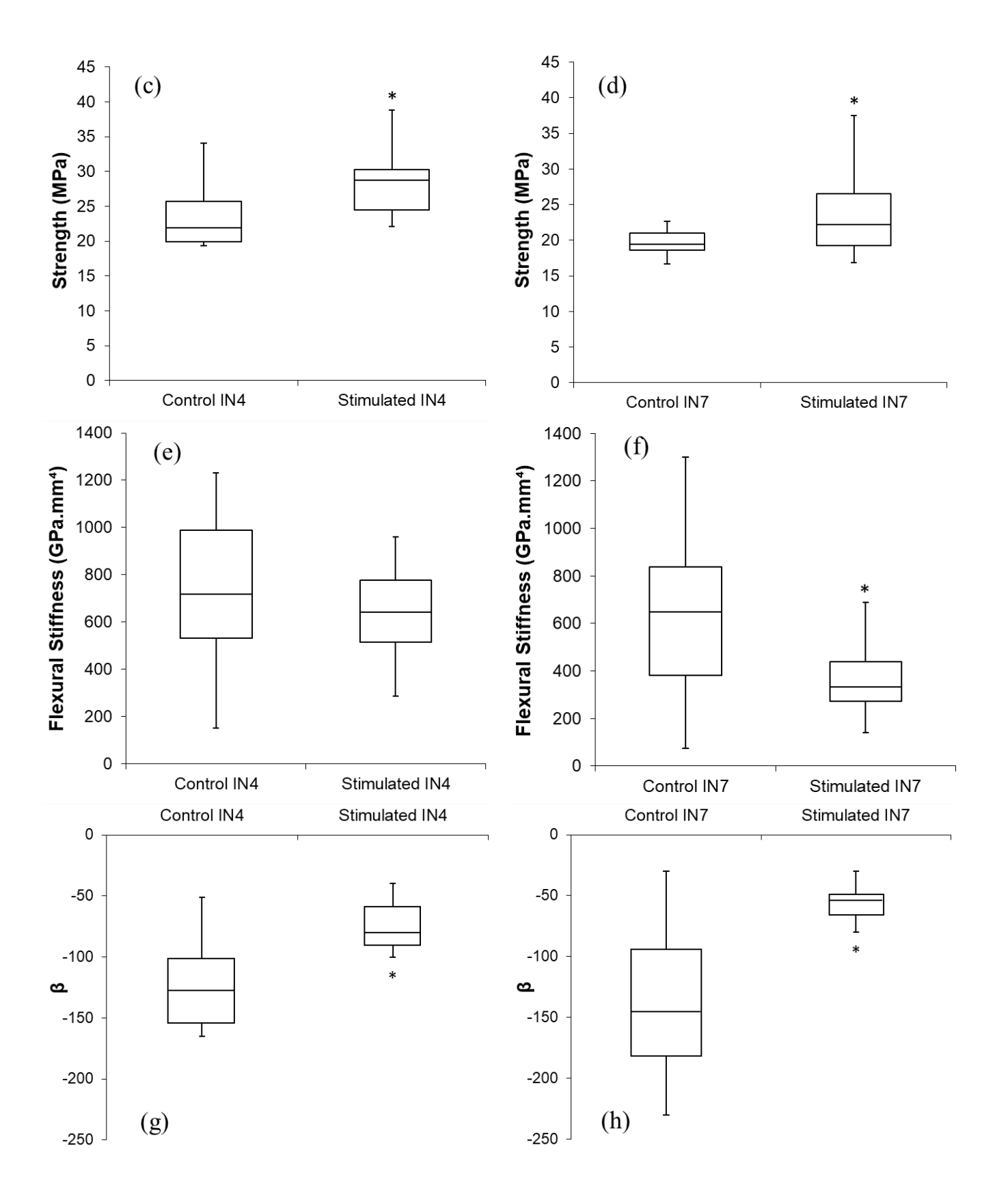


**Figure 8**: Boxplot comparison of control and stimulated plants for internodes 4 and 7 regarding (a-b) elastic modulus, (c-d) strength, (e-f) flexural stiffness, and (g-h)  $\beta$ ; Asterisks (\*) indicate a significant difference between control and stimulated plants at  $\alpha = 0.05$ .

The direction of the mechanical stimulation applied did not affect internode biomechanical properties when tested in a tension versus compression side specific manner. For the elastic modulus and flexural stiffness, there was little difference in the average values between the same-direction bending and the opposite-direction bending (see **Figure S.2** in the Supplemental Document) and no statistically significant differences were identified. (See **Table S.5** in the Supplemental Document).

# 3.3. Comparison of microstructural morphologies between stimulated and non-stimulated plants

Compared to the control, mechanical stimulation appeared to increase the vascular bundle size and density, especially in the outer layer of rind tissue of the younger internode 7 (**Figure 9**). No obvious differences were observed between the compression and tension sides (away from and toward point of stimulation, respectively) of stimulated stems. Increased staining (lignification) of vascular bundles was observed with mechanical stimulation - some of this staining was due to increased development of the sclerenchymatous bundle sheath. Additionally, mechanical stimulation seemed to alter the form of the vascular bundles resulting in greater elongation along the radial axis. Parenchyma cells of the pith, which form the inner part of internodes, also appeared to respond to mechanical stimulation with elevated lignification. Increases in lignin content are often associated with increases in the strength of the tissues [20, 35, 36]. Overall, mechanical stimulation seemed to result in more pronounced changes in the morphology of the rind tissue as compared to the pith tissue. This phenomenon may be due to the mechanical stimulation inducing more severe stresses in the rind than in the pith. However, since the images were not quantified, strong conclusions may not be warranted.

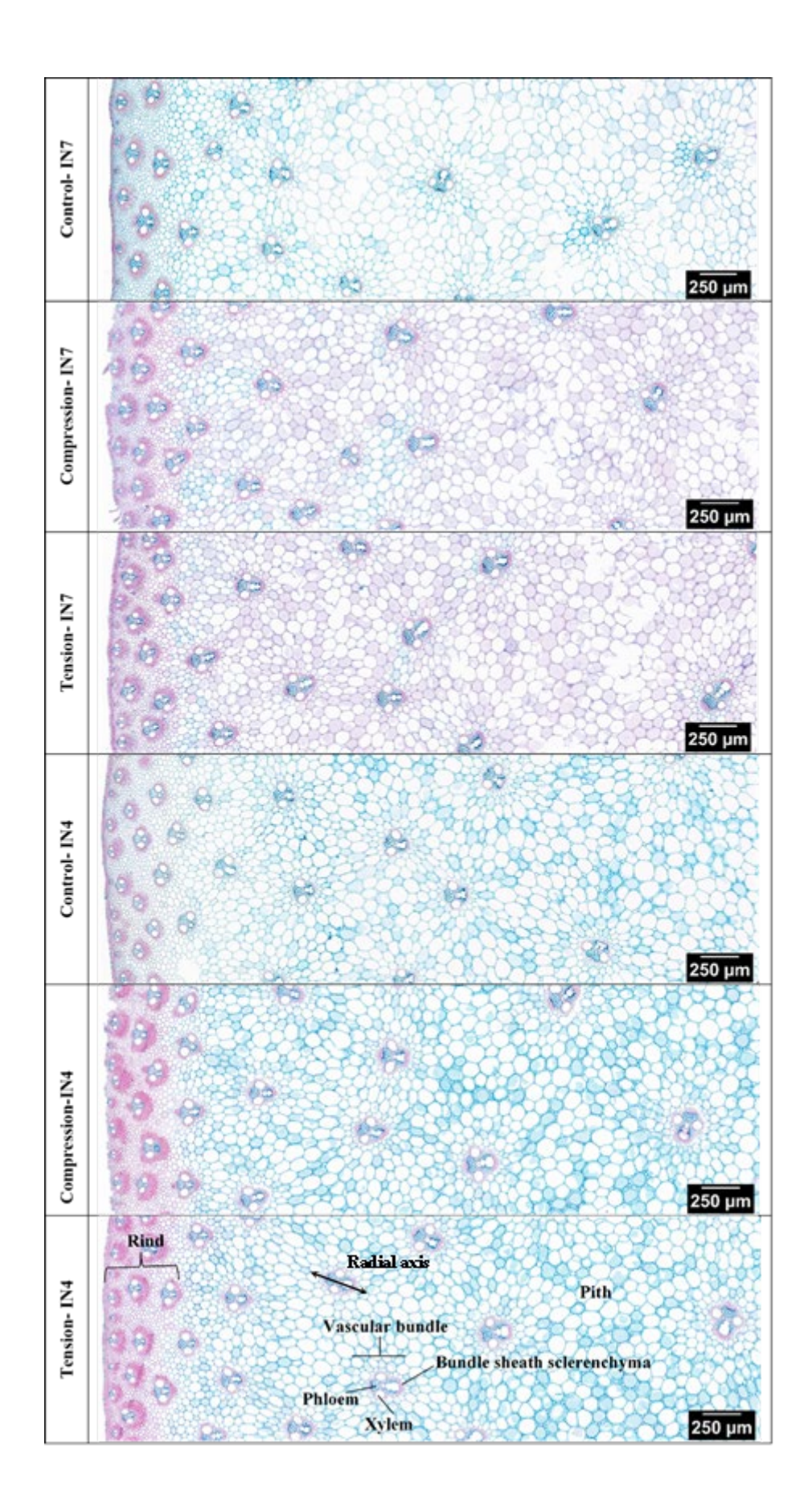


**Figure 9**: Microstructural morphologies of sorghum stem tissues (rind and pith) from control and mechanically stimulated plants (Compression – the side of stem subjected to compression [away from the point of stimulation] and Tension – the side of stem subjected to tension [near the point of stimulation]). The red color in the images indicates lignin accumulation. Young samples (at the time of stimulation) were from internode 7 and more mature samples (at the onset of stimulation) were from internode 4.

#### 4. Discussion

Adaptive growth in plant stems due to mechanical stimulation (thigmomorphogenesis) occurs by activating various regulatory networks, i.e., hormones, proteins, transcription factors, and target genes, and their actions may manifest through altering physiology, morphology, and biomechanical properties. [37-39]. The present study shows that the internodes that were still actively elongating or had just begun elongating at the beginning of mechanical stimulation (younger internodes, i.e., internodes 6-9) experienced more pronounced adaptive growth effects than internodes that were fully or nearly fully elongated (mature internodes, i.e., internodes 2-5). The decrease in the internode lengths with thigmostimulation was greater for the younger internodes. Mechanical stimulation also increased internode diameter, but this effect was not dependent on internode position. From the microstructural morphologies in **Figure 9**, the cell-wall structure reprogramming of the stimulated plants appeared to increase the vascular bundle size and density, especially in the rind tissue of young internodes (internode 7), and to increase lignification of vascular bundles in both pith and rind tissues. These data should be interpreted with caution however, as they remain unquantified. In general, the observations may explain the observed strengthening of the stimulated internodes, as discussed below.

For both internodes 4 and 7, mechanical stimulation increased the force required to cause failure under the four-point bending tests. This result indicates that the stimulated plants can resist higher external loads, which can potentially minimize stem failure due to mechanical loading (e.g., from wind). A similar study by Lemloh et al. [16] on *Sorghum bicolor* found that mechanical stimulation increased the thickness of rind tissue and the bending strength of mature internodes 2 and 3. To understand the higher load bearing ability of the stimulated internodes under bending, several internode physical parameters, e.g., length, diameter, elastic modulus, and strength, were examined. The length and diameter are geometrical parameters, while the modulus and strength are material (tissue) properties. The stimulated internodes exhibited slightly larger diameters compared to the corresponding control internodes which may enhance the resistance to bending owing to an increase in the second moment of area. For internode 7, the stimulated internodes were much shorter than the control internodes, while only modest differences were observed

between the lengths of control and stimulated internode 4. When a fixed magnitude of force is applied to shorter internodes, it results in smaller maximum internal bending moments due to smaller moment arms and hence leads to smaller axial stresses. Thus, the shorter internodes can withstand larger forces before they reach the strength of the internode, i.e., without causing failure. The observed changes in the geometrical parameters of the stimulated internodes contributed to their higher load bearing capacity. The decrease in the internode length and hence the overall reduced height with mechanical stimulation has been demonstrated in several other plants, e.g., *Bryonia dioica*, *Cucumis sativus*, *Ricinus communis* [11], *Brachypodium distachyon* [25] and *Arabidopsis* [15, 40]. Such changes are typically accompanied by an increase of thickness of stems such as in *Phaseolus vulgaris* [41] and Sweetgum. However, in some species the diameter of stimulated stems was reduced, such as in *Arabidopsis* [15] and wheat [42]. As discussed below, the varied responses to mechanical stimulation may result from a variety of factors including the experimental methodology employed and the plant species examined. Our study also showed that younger internodes experienced more pronounced changes in length due to mechanical stimulation compared to the older internodes.

In addition to stem geometry, the biomechanical properties of the tissues can also change due to mechanical stimulation during growth. To assess their changes, we examined the elastic modulus and strength (stress at the onset of failure) of the internodes. For both internodes 4 and 7, the stimulated plants exhibited greater tissue strengths. Overall, these observations indicate that the increase in the load bearing ability of the stimulated internodes was not purely from geometrical changes but also from the strengthening of the tissues themselves. The tissue strengthening likely arises from the observed increased lignification of cell walls in both the pith and rind tissues of stimulated internodes. The stimulated internodes demonstrated reduced elastic moduli for both internodes 4 and 7 when compared to the controls, which indicates that the stimulated internodes had softer (more compliant) tissues. A detailed explanation as to why the mechanical stimulation resulted in more compliant stem tissues is currently lacking. However, previous studies [20, 21] have indicated that a smaller modulus can result from increases in the cell wall microfibril angle (MFA) of the stimulated plants. An increase in the lignin content of mechanically stimulated plants has also been reported in Brachypodium distachyon [25]. This study examined two geographically diverse genotypes (Bd21 and ABR6) which were grown in controlled greenhouse conditions and subjected to mechanical stimulation at the same developmental stage (three tillers). In Bd21, mechanical stimulation decreased the area of both inner and outer vascular bundles, while in ABR6 mechanical stimulation increased the area of vascular bundles. The authors also reported that mechanical stimulation increased the elastic modulus of internodes 2 and 3 for fully mature stems, which the authors associated with reduced stem elongation. For dicot plants, one study observed that mechanical stimulation

resulted in a reduction in elastic modulus, which was found to be correlated with reduced lodging of the stems [25].

When examining the overall stem behavior in bending, flexural stiffness is often used to assess the stem's bending ability. The flexural stiffness is a product of the elastic modulus, which is a tissue property, and the second moment of area, which is a geometrical property. For internode 4, no apparent differences were observed in the flexural stiffness of the stimulated and control internodes. The stimulated internode 4 had a slightly smaller elastic modulus which compensated for the slightly larger second moment of area. However, internode 7 exhibited more pronounced differences in the flexural stiffness between the control and stimulated stems. The stimulated internode 7 showed much lower flexural stiffness, which allows the internode to bend more easily. Gomez et al. [26] reported that field grown lodging-resistant sorghum lines had more compliant tissue, lower flexural stiffness, and stronger stems. Thus, lodging-resistant plants readily deform upon mechanical loading (e.g., from wind) instead of resisting the force. Paul-Victor and Rowe [15] have reported that mechanical stimulation of Arabidopsis decreased the stem flexural stiffness, which the authors attributed to a reduction in pith tissue and lignin content. They also found that mechanical stimulation decreased the density of the lignified cells. Wang et al. [43] studied the influence of mechanical stimulation on the flexural stiffness and biomass content of Corispermum mongolicum plants. They found that mechanical stimulation produced stiffer stems, which was attributed to thicker tissue and higher elastic modulus. The variabilities in flexural stiffness and lignification responses resulting from mechanical stimulation in different species may be due to dissimilar acclimation programs, differences in the tissue composition (i.e.-tissues resulting from secondary growth in some dicots which are not present in monocots) and tissue organization, and/or differences in the nature of the mechanical stimulation applied. Future research reconciling these issues would be beneficial.

The responses of mature internodes to bending applied in the same and opposite directions to the mechanical stimulation applied during growth were also assessed. No statistically significant differences were identified for the elastic modulus, strength, or flexural stiffness of the stimulated internodes when bending in the same and opposite directions from the bending stimulation. These results are consistent with the lack of apparent differences in the morphological features of the tissues subjected to tension and compression during stimulation. It is possible that the amplitude of bending applied during the stimulation was too small to cause significant changes in the development of the tissue between the tension and compression regions. Future work may consider increasing the amplitude of bending deformations during mechanical stimulation to further understand the influence of tensile and compressive stimulation.

Mechanical stimulation promotes changes in the abundances/expression of hormones and genes that can strongly influence the morphology and constituent compositions of cell walls and tissues, which impact the anatomical and biomechanical traits of the stems. A future study investigating how mechanical stimulation-induced changes in hormone abundances and transcriptome expression may be linked to the morpho-anatomical and biomechanical properties of stems would be beneficial.

#### 5. Conclusions

Mechanical stimulation reduced internode elongation and altered the anatomical features of the sorghum stem. The biomechanical properties were also altered by mechanical stimulation: the stimulated internodes had higher strength and lower elastic modulus compared to the control internodes. Younger internodes (at the onset of the stimulation) demonstrated a more pronounced decrease in length due to mechanical stimulation. The changes in the geometrical, morphological, and tissue biomechanical properties induced by mechanical stimulation contributed to increases in the load bearing ability of the stimulated internodes. The changes in the tissue biomechanical properties, i.e., lower elastic modulus, higher strength, and lower flexural stiffness, that contribute to increases in the load bearing ability of the stimulated internodes are consistent with the biomechanical properties of lodging-resistant sorghum genotypes grown in the field. The results provide a foundation for future exploration of the potential for engineering lodging-resistant genotypes tailored to their specific environments, e.g., regions with strong winds.

#### Acknowledgments

This research is sponsored by the National Science Foundation under grant CMMI-1761015. The authors thank Dr. W. Rooney for providing the Della seed used in the study.

#### References

- 1. Bashford, L., et al., *Mechanical properties affecting lodging of sorghum*. Transactions of the ASAE, 1976. **19**(5): p. 962-966.
- 2. Niklas, K.J. and H.-C. Spatz, *Plant physics*. 2012: University of Chicago Press.
- 3. Robertson, D.J., et al., *Corn stalk lodging: a forensic engineering approach provides insights into failure patterns and mechanisms.* Crop Science, 2015. **55**(6): p. 2833-2841.
- 4. Gomez, F.E., et al., *Identifying morphological and mechanical traits associated with stem lodging in bioenergy sorghum (Sorghum bicolor)*. BioEnergy Research, 2017. **10**(3): p. 635-647.
- 5. Ookawa, T., et al., *New approach for rice improvement using a pleiotropic QTL gene for lodging resistance and yield.* Nature communications, 2010. **1**(1): p. 1-11.
- 6. Wu, W. and B.L. Ma, A new method for assessing plant lodging and the impact of management options on lodging in canola crop production. Scientific reports, 2016. **6**(1): p. 1-17.
- 7. Hernández, L.F., *Wind as a mechanical stimulus affect the rate of early reproductive development in sunflower (Helianthus annuus L.)*. International J. Advanced Res. Bot, 2016. **2**: p. 14-24.

- 8. Sparke, M.A. and J.N. Wünsche, *Mechanosensing of Plants*. Horticultural Reviews, 2020. **47**: p. 43-83.
- 9. Boyer, N., Modifications de la croissance de la tige de Bryone (Bryonia dioica) à la suite dirritations tactiles. COMPTES RENDUS HEBDOMADAIRES DES SEANCES DE L ACADEMIE DES SCIENCES SERIE D, 1967. **264**(17): p. 2114-&.
- 10. Meng, S.X., et al., *Reducing stem bending increases the height growth of tall pines*. Journal of Experimental Botany, 2006. **57**(12): p. 3175-3182.
- 11. Jaffe, M.J., *Thigmomorphogenesis: the response of plant growth and development to mechanical stimulation.* Planta, 1973. **114**(2): p. 143-157.
- 12. Jaffe, M., R. Biro, and K. Bridle, *Thigmomorphogenesis: calibration of the parameters of the sensory function in beans.* Physiologia Plantarum, 1980. **49**(4): p. 410-416.
- 13. De Jaegher, G., N. Boyer, and T. Gaspar, *Thigmomorphogenesis in Bryonia dioica: Changes in soluble and wall peroxidases, phenylalanine ammonia-lyase activity, cellulose, lignin content and monomeric constituents.* Plant growth regulation, 1985. **3**(2): p. 133-148.
- 14. Kern, K.A., et al., Mechanical perturbation affects conductivity, mechanical properties and aboveground biomass of hybrid poplars. Tree physiology, 2005. **25**(10): p. 1243-1251.
- 15. Paul-Victor, C. and N. Rowe, *Effect of mechanical perturbation on the biomechanics, primary growth and secondary tissue development of inflorescence stems of Arabidopsis thaliana*. Annals of botany, 2011. **107**(2): p. 209-218.
- 16. Lemloh, M.-L., et al., *Structure-property relationships in mechanically stimulated Sorghum bicolor stalks*. 2014.
- 17. Brulé, V., et al., *Hierarchies of plant stiffness*. Plant Science, 2016. **250**: p. 79-96.
- 18. NIKLAS, K.J., Effects of vibration on mechanical properties and biomass allocation pattern of capsella bursa-pastoris (cruciferae). Annals of Botany, 1998. **82**(2): p. 147-156.
- 19. Brüchert, F. and B. Gardiner, *The effect of wind exposure on the tree aerial architecture and biomechanics of Sitka spruce (Picea sitchensis, Pinaceae)*. American journal of botany, 2006. **93**(10):p. 1512-1521.
- 20. Badel, E., et al., Acclimation of mechanical and hydraulic functions in trees: impact of the thigmomorphogenetic process. Frontiers in Plant Science, 2015. 6: p. 266.
- 21. Telewski, F., *Structure and function of flexure wood in Abies fraseri*. Tree Physiology, 1989. **5**(1): p. 113-121.
- 22. Biddington, N.L., *The effects of mechanically-induced stress in plants—a review*. Plant growth regulation, 1986. **4**(2): p. 103-123.
- 23. Braam, J., *In touch: plant responses to mechanical stimuli*. New Phytologist, 2005. **165**(2): p. 373-389.
- Wu, Q., et al., Touch-induced seedling morphological changes are determined by ethylene-regulated pectin degradation. Science advances, 2020. **6**(48): p. eabc9294.
- 25. Gladala-Kostarz, A., J.H. Doonan, and M. Bosch, *Mechanical stimulation in Brachypodium distachyon: Implications for fitness, productivity, and cell wall properties.* Plant, cell & environment, 2020. **43**(5): p. 1314-1330.
- 26. Gomez, F.E., A.H. Muliana, and W.L. Rooney, *Predicting stem strength in diverse bioenergy sorghum genotypes*. Crop Science, 2018. **58**(2): p. 739-751.
- 27. Lee, S., et al., *Time-dependent mechanical behavior of sweet sorghum stems*. Journal of the Mechanical Behavior of Biomedical Materials, 2020: p. 103731.
- 28. Tolivia, D. and J. Tolivia, *Fasga: a new polychromatic method for simultaneous and differential staining of plant tissues.* Journal of Microscopy, 1987. **148**(1): p. 113-117.
- 29. Köhler, L. and H.-C. Spatz, *Micromechanics of plant tissues beyond the linear-elastic range*. Planta, 2002. **215**(1): p. 33-40.
- 30. Song, R. and A. Muliana, *Modeling mechanical behaviors of plant stems undergoing microstructural changes.* Mechanics of Materials, 2019. **139**: p. 103175.

- 31. Muliana, A., K. Rajagopal, and D. Tscharnuter, *A nonlinear integral model for describing responses of viscoelastic solids*. International Journal of Solids Structures, 2015. **58**: p. 146-156.
- 32. Muliana, A. and K. Rajagopal, *Modeling the response of nonlinear viscoelastic biodegradable polymeric stents*. International Journal of Solids Structures, 2012. **49**(7-8): p. 989-1000.
- 33. Reissner, E., *On one-dimensional finite-strain beam theory: the plane problem.* Zeitschrift für angewandte Mathematik und Physik ZAMP, 1972. **23**(5): p. 795-804.
- 34. Muliana, A., *Large deformations of nonlinear viscoelastic and multi-responsive beams*. International Journal of Non-Linear Mechanics, 2015. 71: p. 152-164.
- 35. Özparpucu, M., et al., Significant influence of lignin on axial elastic modulus of poplar wood at low microfibril angles under wet conditions. Journal of experimental botany, 2019. **70**(15):p. 4039-4047.
- 36. Telewski, F.W., *A unified hypothesis of mechanoperception in plants*. American journal of botany, 2006. **93**(10): p. 1466-1476.
- 37. Samad, A.F., et al., *MicroRNA and transcription factor: key players in plant regulatory network.* Frontiers in plant science, 2017. **8**: p. 565.
- 38. García-Gómez, M.L., E. Azpeitia, and E.R. Álvarez-Buylla, *A dynamic genetic-hormonal regulatory network model explains multiple cellular behaviors of the root apical meristem of Arabidopsis thaliana*. PLoS computational biology, 2017. **13**(4): p. e1005488.
- 39. Dobránszki, J., Application of naturally occurring mechanical forces in in vitro plant tissue culture and biotechnology. Plant Signaling Behavior, 2021. **16**(6): p. 1902656.
- 40. Zhdanov, O., et al., *Wind-evoked anemotropism affects the morphology and mechanical properties of Arabidopsis.* Journal of Experimental Botany, 2021. **72**(5): p. 1906-1918.
- 41. Jaffe, M., *Thigmomorphogenesis: a detailed characterization of the response of beans (Phaseolus vulgaris L.) to mechanical stimulation.* Zeitschrift für Pflanzenphysiologie, 1976. 77(5): p. 437-453.
- 42. Hindhaug, R., M. Bosch, and I.S. Donnison, *Mechanical stimulation in wheat triggers age-and dose-dependent alterations in growth, development and grain characteristics.* Annals of Botany, 2021.
- 43. Wang, Y.H., et al., Brushing effects on the growth and mechanical properties of Corispermum mongolicum vary with water regime. Plant Biology, 2009. 11(5): p. 694-700.

# **Supplemental Document**

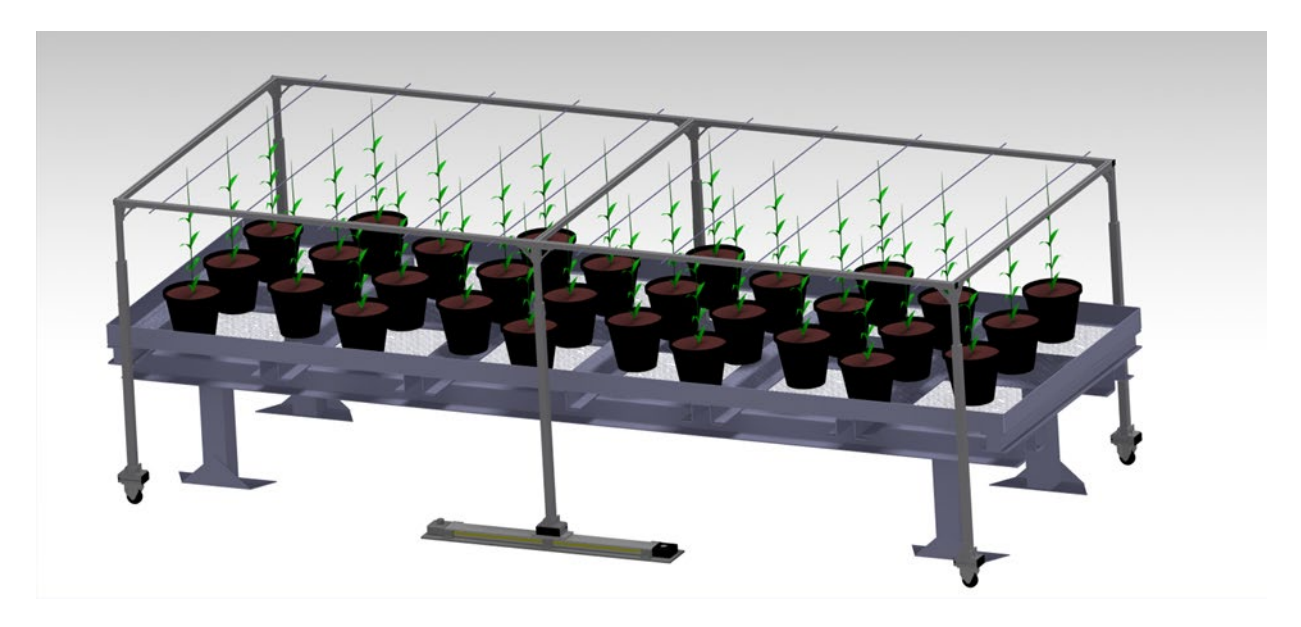
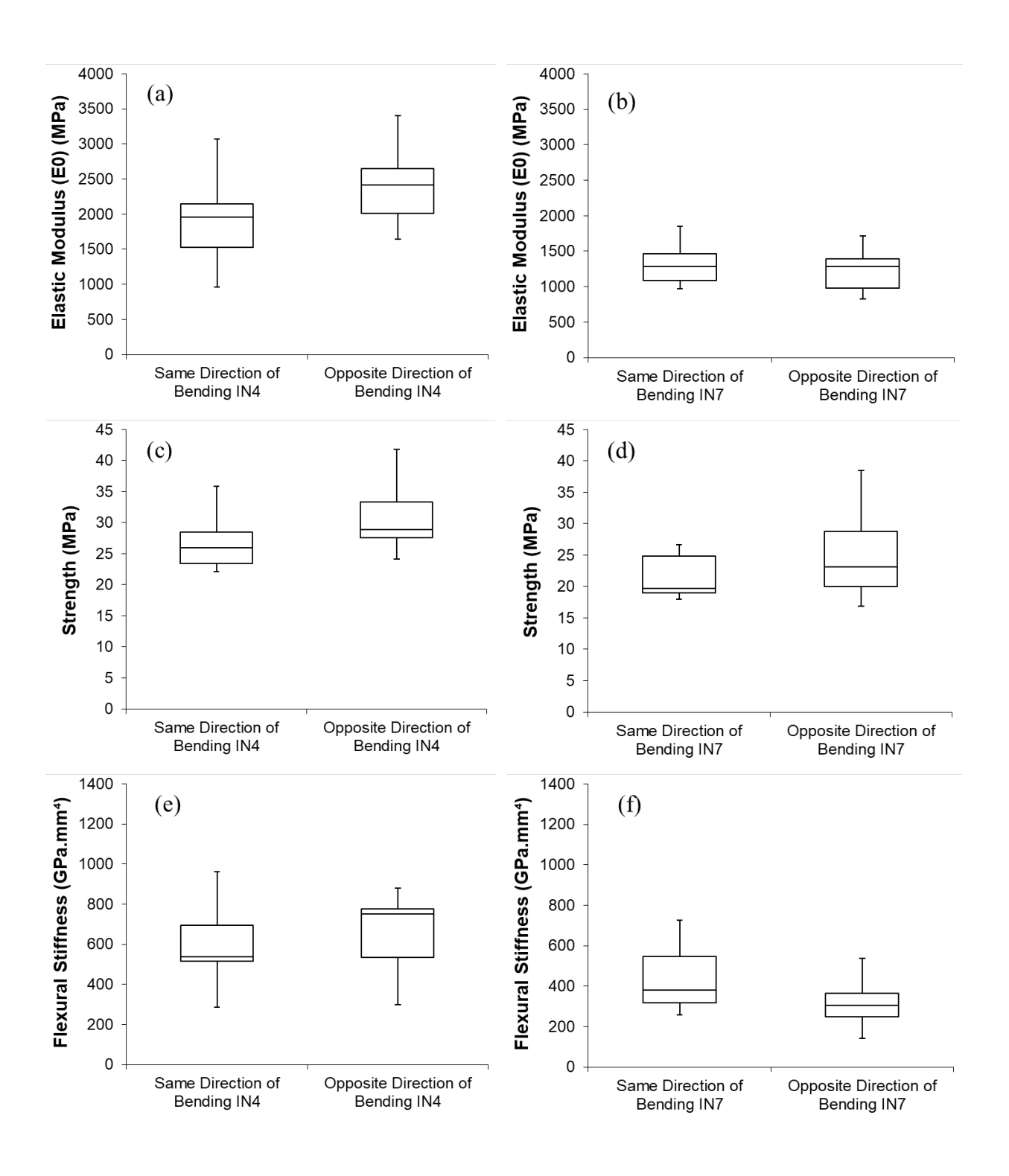
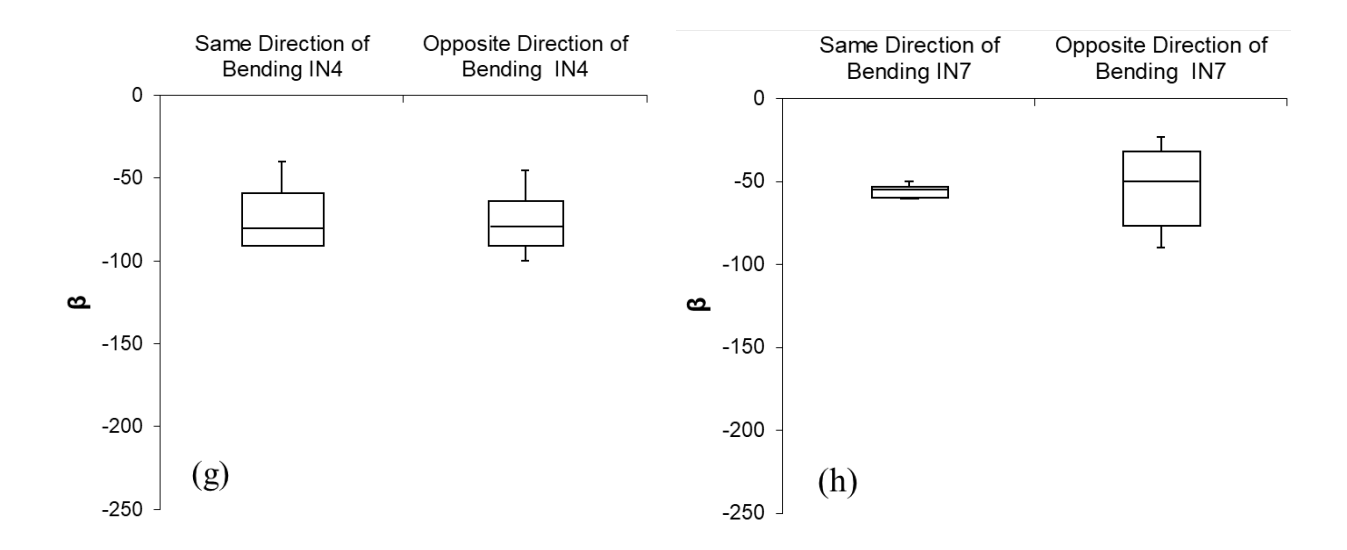


Figure S.1: CAD drawing of the assembly for mechanical stimulation of plants during growth.





**Figure S.2**: Mechanical properties from bending tests administered in the same-direction and opposite-direction of that provided by mechanical stimulation during growth.

**Table S.1**: Statistical comparison of individual internode length between each pair of control and stimulated internodes from unpaired t-test

| Anatomical<br>Traits | Internode<br>No | n<br>(samples from<br>control plants) | n<br>(samples from<br>stimulated plants) | t value | <i>P</i> -value |
|----------------------|-----------------|---------------------------------------|--|---------|-----------------|
|                      | 2               | 16                                    | 16                                       | 0.1341  | 0.8943          |
|                      | 3               | 16                                    | 16                                       | 0.0017  | 0.9986          |
|                      | 4               | 16                                    | 16                                       | 2.9527  | 0.0065          |
| Length               | 5               | 16                                    | 16                                       | 3.3221  | 0.0024          |
| (mm)                 | 6               | 16                                    | 16                                       | 4.5188  | 0.0001          |
|                      | 7               | 16                                    | 16                                       | 6.0070  | < 0.0001        |
|                      | 8               | 16                                    | 16                                       | 7.1345  | < 0.0001        |
|                      | 9               | 16                                    | 12                                       | 7.8342  | < 0.0001        |

**Table S.2**: Two-way ANOVA table of length. The Treatment factor contains two levels: control and stimulated while the Internode factor contains 8 levels: IN2, IN3, IN4, IN5, IN6, IN7, IN8, and IN9. Two-way ANOVA revealed there was a significant interaction effect. Planned contrasts were conducted to further investigate differences in relevant combinations of factor levels.

| Two-way ANOVA-Length |     |                |         |           |  |  |
|----------------------|-----|----------------|---------|-----------|--|--|
|                      | df  | Sum of squares | F value | p value   |  |  |
| Treatment            | 1   | 49985          | 168.196 | < 2.2e-16 |  |  |
| Internode            | 7   | 95978          | 46.137  | < 2.2e-16 |  |  |
| Treatment:Internode  | 7   | 33081          | 15.902  | < 2.2e-16 |  |  |
| Residuals            | 236 | 70136          |         |           |  |  |

| Contrast  | Estimate   | SE         | df  | t ratio    | p value    |
|---|------------|------------|-----|------------|------------|
| Control IN2 - Stimulated IN2                                      | -0.323125  | 6.0949306  | 236 | -0.0530154 | 0.95776451 |
| Control IN3 - Stimulated IN3                                      | -0.075     | 6.0949306  | 236 | -0.0123053 | 0.99019243 |
| Control IN4 - Stimulated IN4                                      | 15.881875  | 6.0949306  | 236 | 2.60575158 | 0.00975    |
| Control IN5 - Stimulated IN5                                      | 18.920625  | 6.0949306  | 236 | 3.10432165 | 0.00214    |
| Control IN6 - Stimulated IN6                                      | 29.731875  | 6.0949306  | 236 | 4.87813184 | 1.97E-06   |
| Control IN7 - Stimulated IN7                                      | 43.491875  | 6.0949306  | 236 | 7.13574573 | 1.18E-11   |
| Control IN8 - Stimulated IN8                                      | 59.569375  | 6.0949306  | 236 | 9.77359366 | 3.66E-19   |
| Control IN9 - Stimulated IN9                                      | 63.4333333 | 6.58327746 | 236 | 9.63552481 | 9.64E-19   |
| (Control IN6 - Stimulated IN6) + (Control IN7 - Stimulated IN7)   | 38.4       | 12.2       | 236 | 3.152      | 0.0018     |
| - (Control IN4 - Stimulated IN4) - (Control IN5 - Stimulated IN5) |            |            |     |            |            |
| (Control IN8 - Stimulated IN8) + (Control IN9 - Stimulated IN9)   | 49.8       | 12.4       | 236 | 4.001      | 0.0001     |
| - (Control IN6 - Stimulated IN6) - (Control IN7 - Stimulated IN7) |            |            |     |            |            |

**Table S.3**: Two-way ANOVA table of diameter and second moment of area comparison (SMOA). The Treatment factor contains two levels: control and stimulated while the Internode factor contains 8 levels: IN2, IN3, IN4, IN5, IN6, IN7, IN8, and IN9.

| Two-way ANOVA-Diameter |     |                |         |          |  |  |
|------------------------|-----|----------------|---------|----------|--|--|
|                        | df  | Sum of squares | F value | p value  |  |  |
| Treatment              | 1   | 6.995          | 10.3937 | 0.001444 |  |  |
| Internode              | 7   | 16.049         | 3.4068  | 0.001737 |  |  |
| Treatment:Internode    | 7   | 1.288          | 0.2734  | 0.963809 |  |  |
| Residuals              | 235 | 158.149        |         |          |  |  |

| Two-way ANOVA-SMOA  |     |                |         |          |  |  |
|---------------------|-----|----------------|---------|----------|--|--|
|                     | df  | Sum of squares | F value | p value  |  |  |
| Treatment           | 1   | 91817          | 9.3286  | 0.002516 |  |  |
| Internode           | 7   | 227849         | 3.3071  | 0.002245 |  |  |
| Treatment:Internode | 7   | 20061          | 0.2912  | 0.956967 |  |  |
| Residuals           | 235 | 2312983        |         |          |  |  |

Table S.4: Statistical analysis comparing the mechanical properties of stimulated and control plants

| Property  | Internode<br>No | n<br>(samples from<br>control plants) | n<br>(samples from<br>stimulated plants) | t value | <i>P</i> -value |
|-----------|-----------------|---------------------------------------|--|---------|-----------------|
| $E_{0}$   | 4               | 12                                    | 14                                       | 2.1436  | 0.0443          |
| $L_0$     | 7               | 12                                    | 15                                       | 4.4961  | 0.0007          |
| Strength  | 4               | 9                                     | 13                                       | -2.6067 | 0.0178          |
| 8         | 7               | 11                                    | 15                                       | -2.3230 | 0.0314          |
| Flexural  | 4               | 12                                    | 14                                       | 0.9474  | 0.3561          |
| Stiffness | 7               | 12                                    | 15                                       | 2.2743  | 0.0385          |
| В         | 4               | 12                                    | 14                                       | -4.6142 | 0.0003          |
| P         | 7               | 12                                    | 15                                       | -4.4920 | 0.0006          |

**Table S.5**: Statistical analysis comparing the effects of the bending direction on the mechanical properties of internodes in Figure S.2

| Mechanical properties | Internode<br>No | n<br>(Same Direction of<br>Bending) | n<br>(Opposite Direction<br>of Bending) | t value  | <i>P</i> -value |
|-----------------------|-----------------|-------------------------------------|---|----------|-----------------|
| $E_0$ (MPa)           | 4               | 7                                   | 7                                       | 1.2641   | 0.2317          |
| $L_0$ (MI a)          | 7               | 7                                   | 8                                       | - 0.5488 | 0.5927          |
| Strength              | 4               | 6                                   | 7                                       | 1.1999   | 0.2554          |
|                       | 7               | 7                                   | 8                                       | 1.1659   | 0.2692          |
| Flexural              | 4               | 7                                   | 7                                       | 0.4065   | 0.6915          |
| Stiffness             | 7               | 7                                   | 8                                       | -1.4826  | 0.1662          |
| β                     | 4               | 7                                   | 7                                       | -0.7211  | 0.4847          |
| P                     | 7               | 7                                   | 8                                       | 0.74964  | 0.4671          |

#### Nonlinear viscoelastic beam formulation

This section discusses the formulation of the four-point bending model to simulate the bending tests of sorghum internodes. Consider a straight prismatic beam, in its undeformed configuration, whose centroidal axis is placed along the x-axis of the Cartesian coordinate system (**Fig. S.3**). The x-y plane is the plane of symmetry with regards to the applied transverse load and transverse deformation, and the z-axis is the out of plane axis. We follow the kinematics of the deformed beam, discussed in Reissner (1972). It is assumed that the plane that is perpendicular to the centroidal axis of the undeformed beam remains plane during the deformation. We neglect stretching in the lateral directions of the beam and neglect the transverse shear deformations.

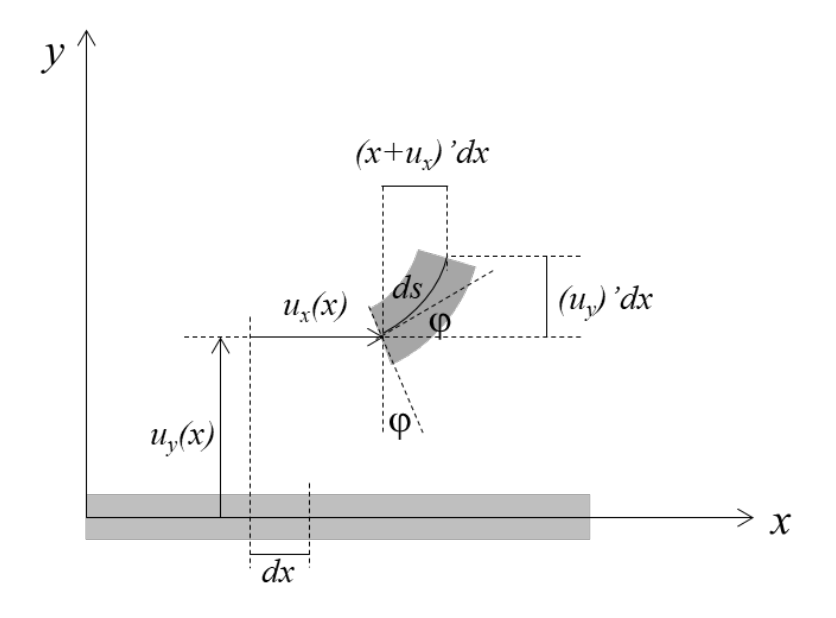


Figure S.3: A schematic of a straight prismatic beam, in its undeformed configuration

Consider a material point with the position defined by  $\mathbf{r}_o = x\mathbf{i}$ , and its current position during the deformation is  $\mathbf{r} = (x + u_{xo}(x))\mathbf{i} + u_{yo}(x)\mathbf{j}$ , where  $u_{xo}(x)$  and  $u_{yo}(x)$  are the scalar components of the displacement of a material point located along the centroidal axis of the beam in the x and y directions, respectively; and  $\mathbf{i}$  and  $\mathbf{j}$  are the unit basis vectors along the x and y axes, respectively. For a differential beam element, whose initial length is dx, and the current length along its centroidal axis is ds, the engineering axial strain is given by  $\varepsilon_{xo} = \frac{ds - dx}{dx}$ . The rotational angle of the material point in the deformed configuration is  $\varphi$ , which is expressed by:

$$\cos \varphi = \frac{1 + \frac{du_{xo}}{dx}}{1 + \varepsilon_{xo}}; \qquad \sin \varphi = \frac{\frac{du_{yo}}{dx}}{1 + \varepsilon_{xo}}$$
(S.1)

Hence the displacement gradients are written as:

$$\frac{du_{xo}}{dx} = (1 + \varepsilon_{xo})\cos\varphi - 1; \qquad \frac{du_{yo}}{dx} = (1 + \varepsilon_{xo})\sin\varphi \tag{S.2}$$

With the assumption that a plane that is perpendicular to the longitudinal axis of the beam remains plane during the deformation, the axial strain at any distance y from the centroidal axis is:

$$\varepsilon_{xx} = \varepsilon_{xo} - y\varphi'; \quad \kappa_z = \varphi'$$
 (S.3)

It is noted that  $\kappa_z$  is the curvature of the deformed beam.

The axial stresses,  $\sigma_{xx}$ , arise due to the internal axial force and bending moment in the beam. Since the formulation of beam in-plane bending involves only axial stress  $\sigma_{xx}$ , axial strain  $\varepsilon_{xx}$ , and a single curvature  $\kappa_{z}$ , in the rest of the manuscript we will drop the indices for the field variables and consider

$$\sigma = \sigma_{xx}, \ \varepsilon = \varepsilon_{xx}, \ \kappa = \kappa_z, \ u = u_{xo}, \ v = u_{yo}$$

Let N and M be the internal axial force and bending moment, respectively, and A be the cross-sectional area of the beam. Imposing the equilibrium conditions results in:

$$N = \int_{A} \sigma dA; \qquad M = -\int_{A} y \sigma dA \tag{S.4}$$

A constitutive relation is needed to relate the force and moment to the deformations of the beam. In case of bending, the outer surfaces (top and bottom sections) of the beam will be under the most severe axial stress and strain. To determine a suitable constitutive material model for the stem under bending, we conducted limited uniaxial tensile tests of rind tissues of Della genotypes from mature and young internodes (**Fig. S.4**). It is noted that these rind tissues were grown in a greenhouse at a different time. The purpose of presenting these uniaxial tensile tests is simply to show the nonlinear stress-strain responses of the tissue prior to failure and the relatively small strain level prior to failure (less than 10% strain).

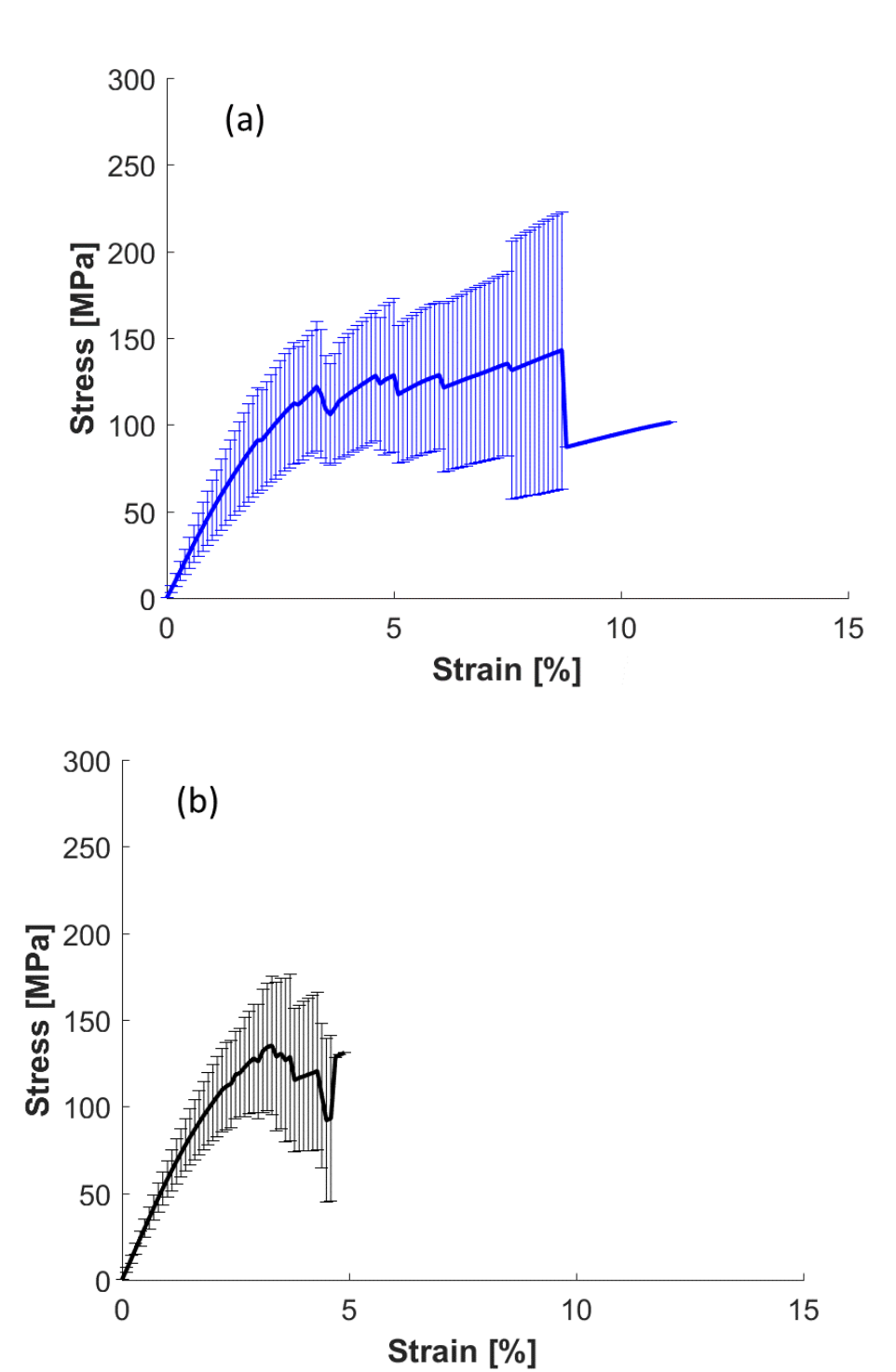


Figure S.4: Uniaxial tensile responses of rind tissues of (a) mature internodes and (b) young internodes

The following constitutive model is used to describe the nonlinear stress-strain responses of the tissue:

$$\sigma = \frac{E_0}{\beta} \left( e^{\beta |\varepsilon|} - 1 \right) \frac{\varepsilon}{|\varepsilon|} \tag{S.5}$$

The tension and compression responses are assumed to be the same. Substituting the model in Eq. (A.5) to the equilibrium Eq. (A.4) with N=0 and hence  $\varepsilon_{xo}=0$ , and assuming a circular cross-section of the stem internode with a radius r and  $dA=2\sqrt{r^2-y^2}\,dy$ , we have:

$$-\int_{-r}^{r} \frac{E_0}{\beta} \left( e^{\beta |y\kappa(x)|} - 1 \right) \operatorname{sgn}(\varepsilon) \left( 2\sqrt{r^2 - y^2} \right) dy = M(x)$$

$$2\int_{0}^{r} \frac{E_0}{\beta} \left( e^{\beta |y\kappa(x)|} - 1 \right) \left( 2\sqrt{r^2 - y^2} \right) dy = M(x)$$
(S.6)

We use a finite difference method to solve Eq. (A.6) in simulating the four-point bending deformation. The beam has a length L and two lateral forces of magnitude P are prescribed at a distance a from the end supports. Due to symmetry, only half of the beam length is modeled. The beam is spatially discretized along its centroidal axis with the incremental length of  $\Delta x$ , and the location of each material point is given as  $x_i = i\Delta x$ ,  $i = 0,1,...N_{L/2}$ . At each location  $x_i$ , the beam is discretized along its lateral axis y,  $y_j = j\Delta y$ ,  $j = 0,1,...N_r$ . At each location  $x_i$ , the internal bending moment  $M_i$  is known, i.e.,  $Px_i$ ,  $i < N_P$ 

$$M_i = \begin{cases} Px_i, & i < N_P \\ Pa, & i \ge N_P \end{cases}$$
, where  $N_P$  is the number of the discretized segment at which the load  $P$  is

prescribed. The corresponding curvature  $\kappa_i$  is then obtained iteratively from Eq. (A.6), and the Newton-Raphson method is used to minimize the residual. The residual is defined as:

$$R = 2\frac{E_0}{\beta} \sum_{i=0}^{N_r} \left( e^{\beta |y_j \kappa_i|} - 1 \right) \left( 2\sqrt{r^2 - y_j^2} \right) y_j \Delta y - M_i$$
 (S.7)

The initial trial for the curvature is  $\kappa_i^{(0)} = \kappa_{i-1}$  and  $\kappa_0 = 0$ , and the curvature is then obtained from:

$$\kappa_i^{(p+1)} = \kappa_i^{(p)} - \left(\frac{dR^{(p)}}{d\kappa_i}\right)^{-1} R^{(p)}$$
(S.8)

where p is the iteration counter. The converged value for  $\kappa_l$  is obtained when  $|R| \leq Tol$ . Once the curvature has been determined, the rotational angle, axial displacement, and lateral displacement can be determined with boundary conditions ( $\varphi_{N_{L/2}} = u_0 = v_0 = 0$ ):

$$\varphi_{i+1} = \kappa_i \Delta x + \varphi_i$$

$$u_{i+1} = (\cos \varphi_{i+1} - 1) \Delta x + u_i$$

$$v_{i+1} = \sin \varphi_{i+1} \Delta x + v_i$$
(S.9)

The sorghum stem tissues experience viscoelastic responses, as shown in Fig. S.5.

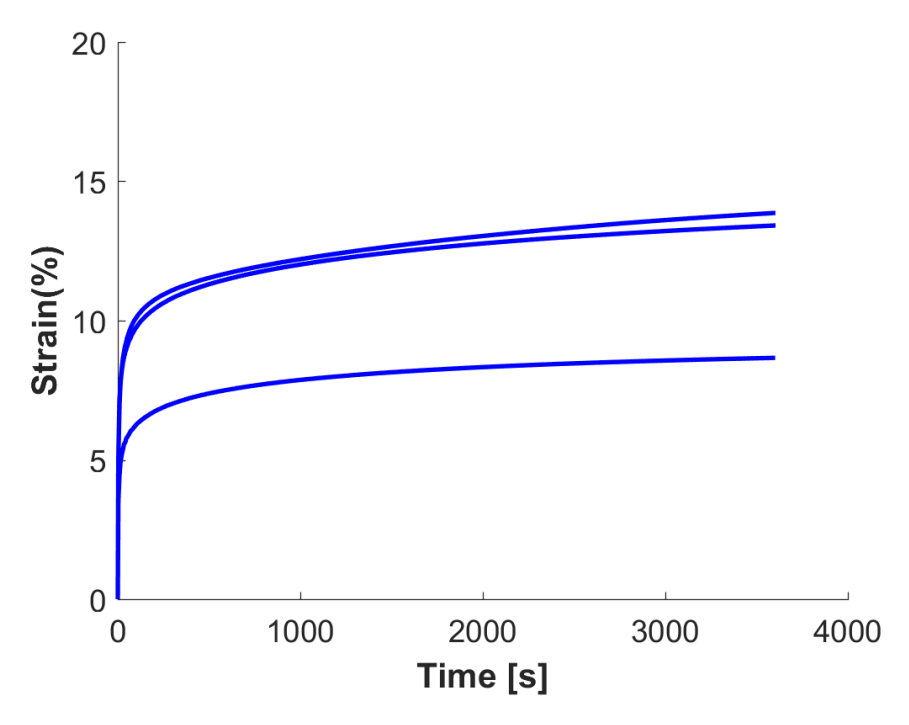


Figure S.5: Viscoelastic responses of rind tissues of mature internodes

To incorporate the viscoelastic deformation, a nonlinear quasi-linear viscoelastic model (Muliana et al. 2015) is adopted, and Eq. (A.6) is now rewritten as:

$$2\int_{0}^{r} \frac{E_{0}}{\beta} \left(e^{\beta|y\kappa(x)|} - 1\right) \left(2\sqrt{r^{2} - y^{2}}\right) dy = \underbrace{M(x,0) J(t) + \int_{0}^{t} J(t-s) \frac{dM(x,s)}{ds} ds}_{H(x,t)}$$
(S.10)

In simulating the four-point bending creep tests, at each instance of time the right-hand side is known as the history of internal bending moment, which is known:

$$M(x,t) = \begin{cases} \alpha tx, & 0 \le t \le t_P, 0 \le x \le a \\ \alpha ta, & 0 \le t \le t_P, a < x \le L/2 \\ Px, & t > t_P, 0 \le x \le a \\ Pa, & t > t_P, a < x \le L/2 \end{cases}$$
(S.11)

where  $P = \alpha t_P$ ,  $\alpha$  is the loading rate and  $t_P$  is the rise time, i.e., the time needed to load the specimen to the creep load. From Eq. (A.11) the rate of moment is a constant  $C^*$ :

$$\frac{dM(x,t)}{dt} = \begin{cases}
\alpha x, & 0 \le t \le t_P, 0 \le x \le a \\
\alpha a, & 0 \le t \le t_P, a < x \le L/2 \\
0, & t > t_P, 0 \le x \le a \\
0, & t > t_P, a < x \le L/2
\end{cases}$$
(S.12)

A finite difference method is also used to solve Eq. (A.10). In addition to the spatial discretization discussed above, a temporal discretization is needed, which is  $t_k = k\Delta t$ , k = 0, 1, 2, ... The discretized form of the right-hand side of Eq. (A.10) is

$$H_{i}^{k} = H(x,t) = M_{i}^{0} J(t_{k}) + \int_{0}^{t_{k}} J(t-s) \frac{dM_{i}^{s}}{ds} ds$$
(S.13)

The kernel time in Eq. (A.12) is modeled with a Prony series,  $J(t) = J_0 + \sum_{n=1}^{M_P} J_n \left(1 - e^{-t/\tau_n}\right)$ , and with a constant rate of moment in Eq. (A.12) and M(x,0) = 0, Eq. (A.13) is rewritten as:

$$H_{i}^{k} = C * \int_{0}^{t_{k}} J(t-s)ds = C * \left[ J_{0}t_{k} + \sum_{n=1}^{M_{p}} J_{n} \left( t_{k} - \tau_{n} e^{-(t-t_{k})/\tau_{n}} + \tau_{n} e^{-t/\tau_{n}} \right) \right]$$
(S.14)

Similar to the time-independent behavior, Eq. (A.10) will be solved iteratively to determine the temporal and spatial dependent curvature  $\kappa_i^k$ . The residual is defined as:

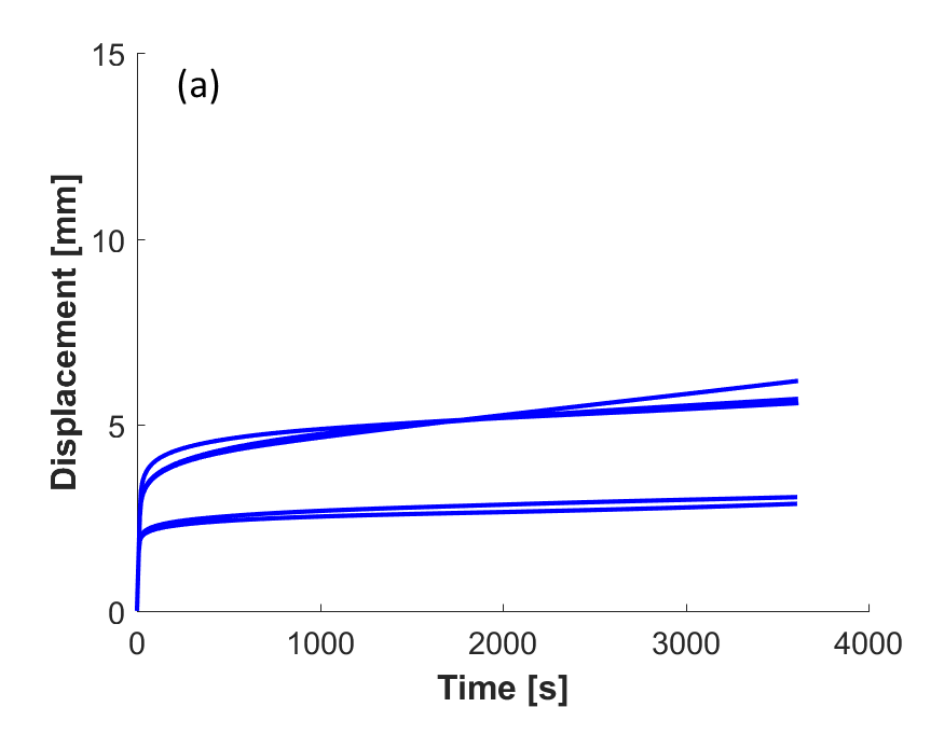
$$R = 2\frac{E_0}{\beta} \sum_{j=0}^{N_r} \left( e^{\beta |y_j \kappa_i^k|} - 1 \right) \left( 2\sqrt{r^2 - y_j^2} \right) y_j \Delta y - H_i^k$$
(S.15)

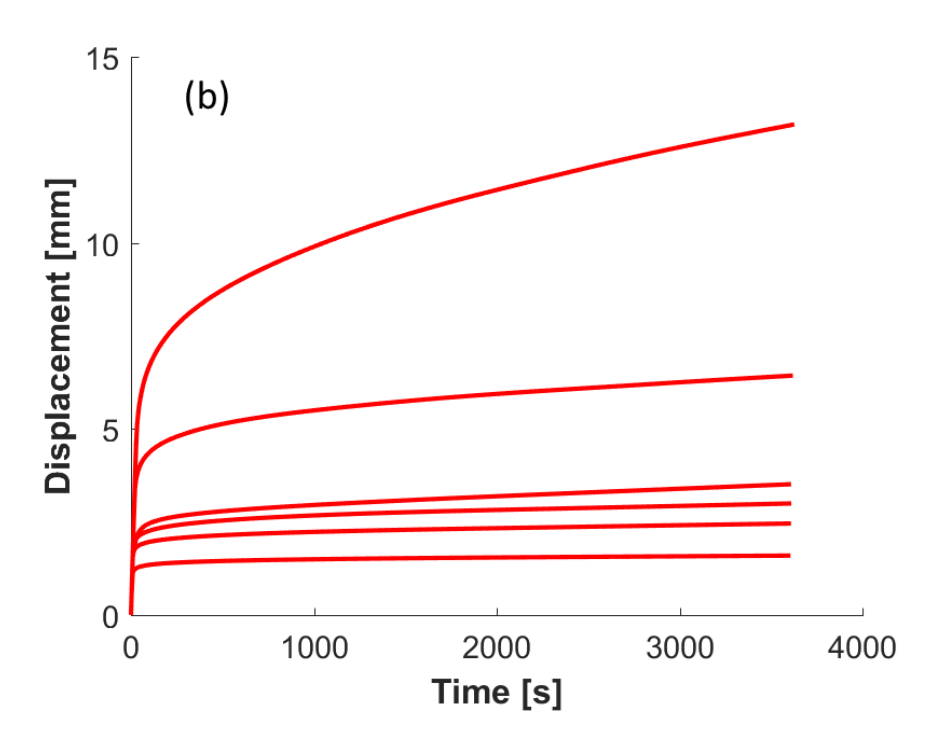
The same procedure in Eqs. (A.8) and (A.9) is then followed to obtain the curvature, rotational angle, axial displacement, and lateral displacement.

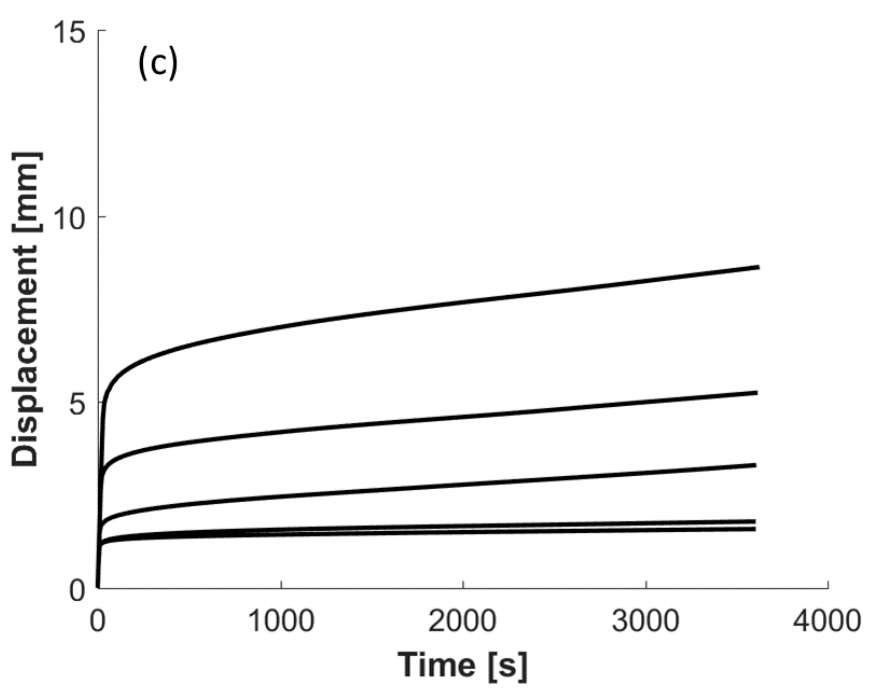
## **Creep bending tests**

Creep tests under four-point bending were also conducted on internodes 4 and 7 from control and stimulated plants. A constant force of 50% of the average maximum bending force was applied during the creep tests for 1 hour. The maximum bending force for control and stimulated plants was different for each internode, and hence the creep stress level for each group varied. The applied creep stress levels for internodes 4 and 7 of control plants were 0.032 N and 0.024 N, respectively, while the stress levels for internodes 4 and 7 of the stimulated plants were 0.048 N and 0.046 N, respectively.

Creep bending tests were also performed to evaluate the time-dependent behavior of both control and stimulated plants and to compare the groups. **Figure S.6** shows the time-dependent lateral displacements from the four-point bending tests. Creep behaviors were observed in all specimens. It is noted that only a small number of samples (5-6 samples for each of control and stimulated internode) were available for the creep tests. A normalized creep function, discussed in Section 2.7, with four terms (N=4) was used to capture the creep responses.







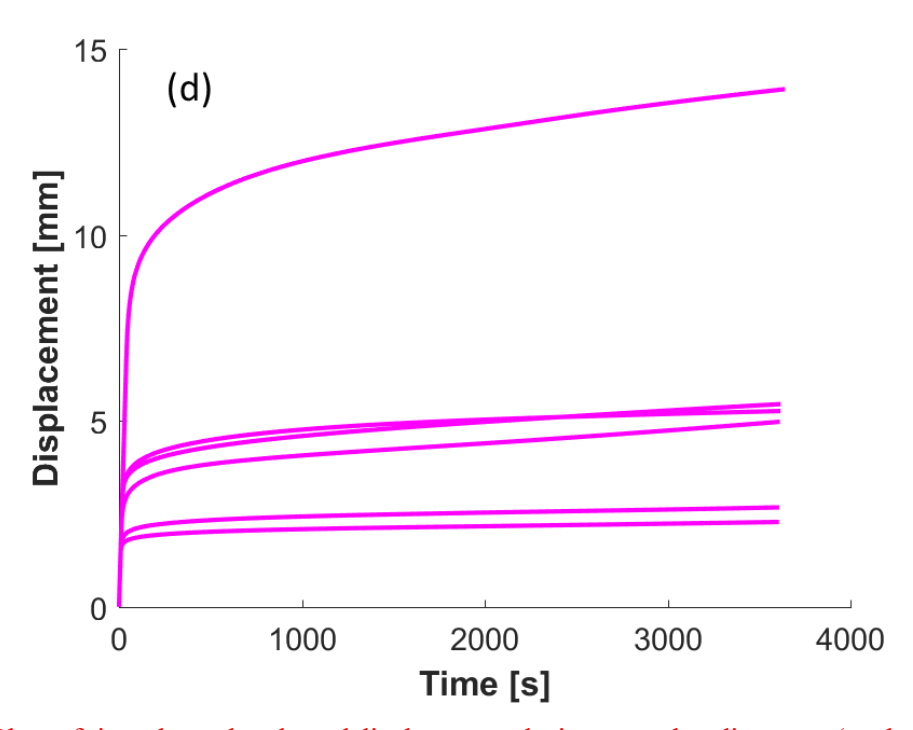


**Figure S.6**: Plots of time-dependent lateral displacement during creep bending tests (each trace is a unique stem sample): (a) control internode 4, (b) stimulated internode 4, (c) control internode 7, and (d) stimulated internode 7.

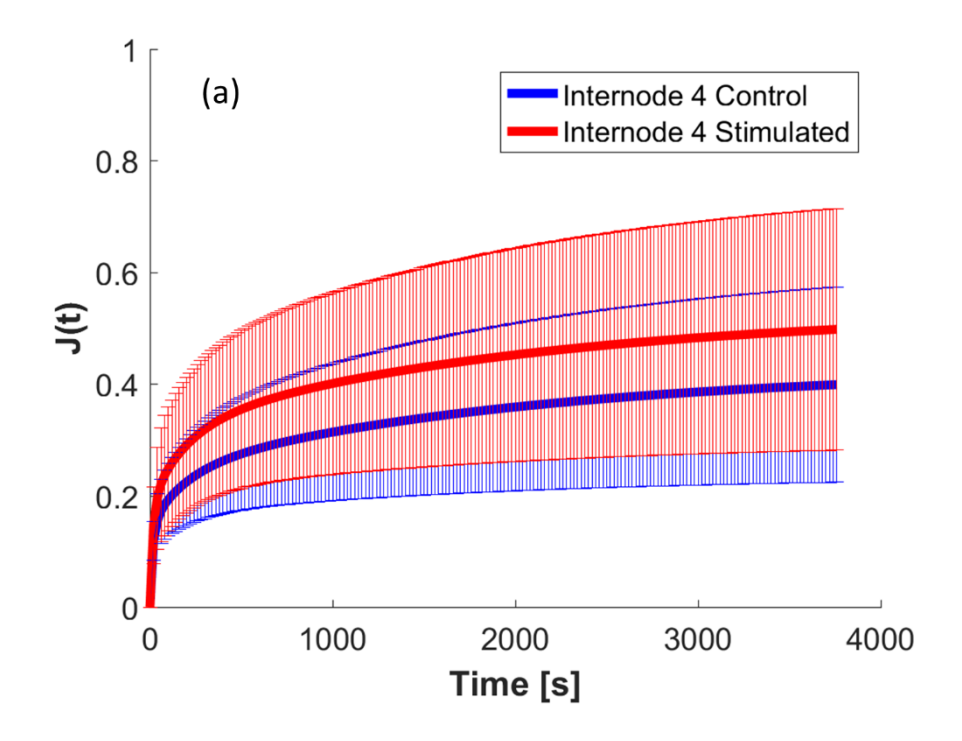
From the creep response, the normalized time-dependent creep function—was calibrated. These calibrated properties were used to reveal whether the tissue's mechanical properties were altered by the mechanical stimulation. **Table S.6** shows the calibrated material parameters from the creep tests. These calibrated values from the creep tests were generally consistent with the values obtained from the quasistatic bending tests, indicating that the chosen nonlinear material model can adequately capture the physical properties of the stem. The parameters  $J_1 - J_4$  denote the weighting factors for the four time scales,  $\tau_1$ - $\tau_4$  ( $\tau_1$ =2,  $\tau_2$ =20,  $\tau_3$ =200, and  $\tau_4$ =2000 seconds) in a creep spectrum, which represent the relative dominance of the response at different times.

Table S.6: Material parameters and time dependent properties for control and stimulated plants under creep bending ( $J_{1-4}$  are normalized creep functions)

| Internode<br>Number | $E_0$ (MPa) (Avg $_{\pm}$ SD) | $\beta$ (Avg $\pm$ SD) | $J_1$ (Avg $\pm$ SD) | $J_2$ (Avg $\pm$ SD) | $J_3$ (Avg $\pm$ SD) | $J_4$ (Avg $_{\pm}$ SD) |
|---------------------|-------------------------------|------------------------|----------------------|----------------------|----------------------|-------------------------|
|---------------------|-------------------------------|------------------------|----------------------|----------------------|----------------------|-------------------------|

| Control<br>Plants    | 4 | 3520 ± 1592.4 | -132±93.05 | 0.041 ±<br>0.017 | 0.106±<br>0.053 | 0.094±<br>0.032 | 0.186±<br>0.115  |
|----------------------|---|---------------|------------|------------------|-----------------|-----------------|------------------|
|                      | 7 | 2896±1252.29  | -107±91.40 | 0.040±<br>0.019  | 0.085±<br>0.021 | 0.077±<br>0.019 | 0.257±<br>0.130  |
| Stimulated<br>Plants | 4 | 2482 ± 726.28 | -67±41.079 | 0.038±<br>0.015  | 0.148±<br>0.091 | 0.132±<br>0.023 | 0.212±<br>0.118  |
|                      | 7 | 1676±595.83   | -89±48.772 | 0.038±<br>0.027  | 0.072±<br>0.030 | 0.074±<br>0.042 | 0.111 ±<br>0.079 |

The time-dependent compliances, shown in **Figure S.7**, from the control and stimulated plants were similar for both internode 4 and internode 7. It should be noted that only a small number of samples were available to perform the creep tests. Regardless, all the internodes demonstrated creep responses. The statistical analysis for time-dependent compliances are included in **Table S.7**. Individual time-dependent compliances for all the tested samples of internodes 4 and 7 are shown in **Figure S.8**.



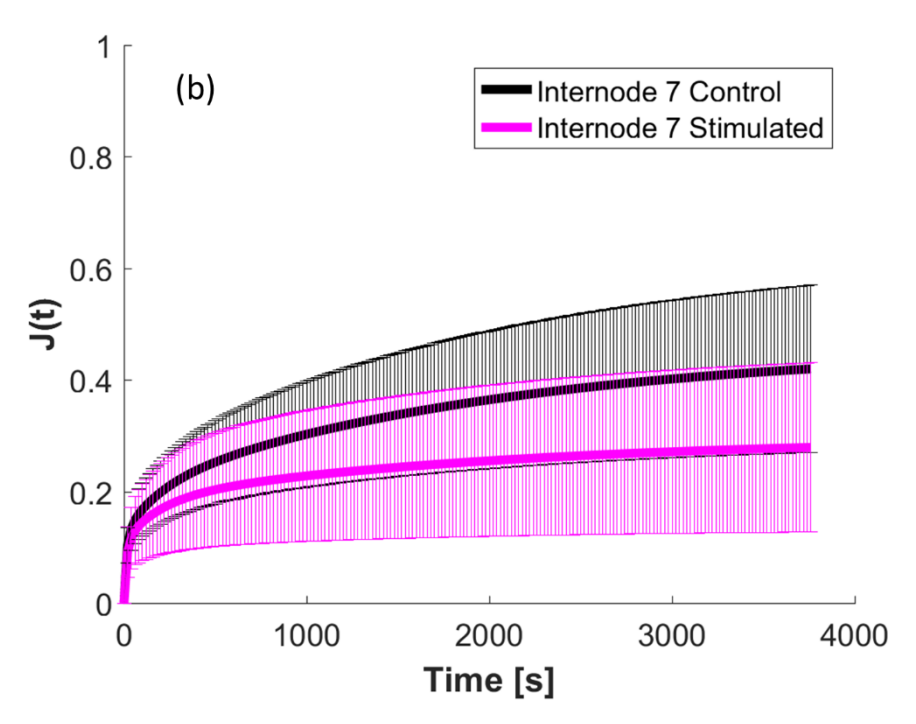
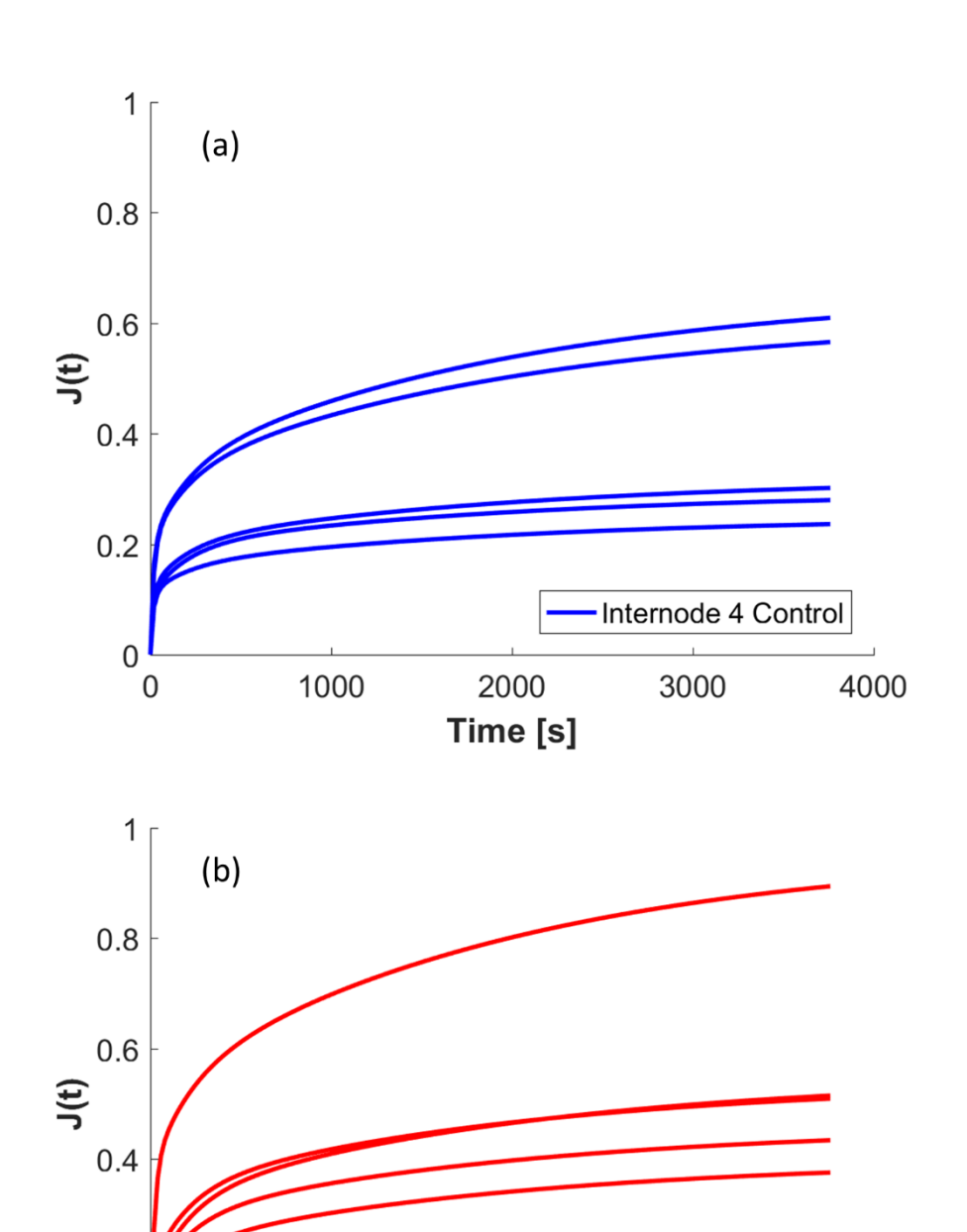


**Figure S.7**: A comparison between control and stimulated plants for internodes 4 and 7 with regards to the time-dependent parameter J(t): (a) control and stimulated internode 4, (b) control and stimulated internode 7; data are means  $\pm$  SD.



Internode 4 Stimulated

0.2

Time [s]

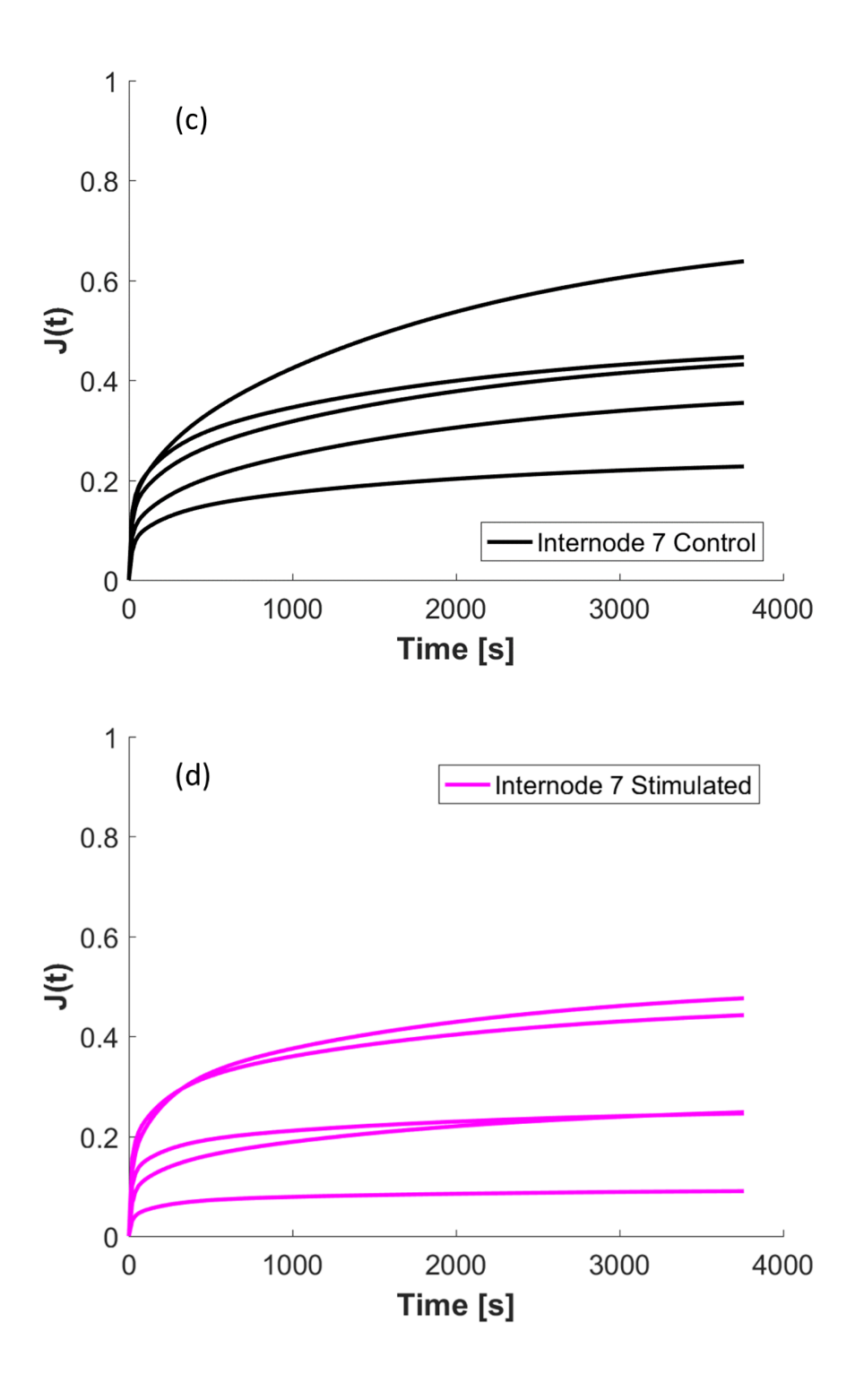


**Figure S.8:** A comparison between control and stimulated plants for internodes 4 and 7 with regards to the time-dependent parameter J(t) (each trace is a unique stem sample): (a) control internode 4, (b) stimulated internode 4, (c) control internode 7, and (d) stimulated internode 7.

**Table S.7**: Statistical analysis comparing stem creep bending parameters between stimulated and control plants (it reveals that no significant differences existed between the parameters from the control and stimulated plants except for  $J_4$ )

| Mechanical properties        | Internode<br>No | n (Control) | n (Stimulated) | t value | <i>P</i> -value |
|------------------------------|-----------------|-------------|----------------|---------|-----------------|
| $E_0$ (MPa)                  | 4               | 5           | 6              | 1.1726  | 0.2837          |
|                              | 7               | 5           | 6              | 2.2591  | 0.0538          |
| β                            | 4               | 5           | 6              | -1.4465 | 0.2045          |
|                              | 7               | 5           | 6              | -0.2064 | 0.8453          |
| $J_{_1}$                     | 4               | 5           | 6              | 0.2778  | 0.7881          |
|                              | 7               | 5           | 6              | 0.1337  | 0.8966          |
| $J_2$                        | 4               | 5           | 6              | -0.9433 | 0.3705          |
|                              | 7               | 5           | 6              | 0.8336  | 0.4267          |
| $J_3$                        | 4               | 5           | 6              | -2.1914 | 0.0637          |
|                              | 7               | 5           | 6              | 0.5418  | 0.6041          |
| ${J}_{\scriptscriptstyle 4}$ | 4               | 5           | 6              | -0.4515 | 0.6634          |
|                              | 7               | 5           | 6              | 2.4062  | 0.0423          |

Creep tests revealed viscoelastic responses for all internodes. It is interesting to note that both control internodes 4 and 7 had similar time-dependent characteristics, suggesting that the viscoelastic properties of these internodes were equivalent without mechanical stimulation. It is noted that only a small number of samples (5-6) were used in creep tests. While the preliminary results are interesting, further investigation is needed to fully explain such behaviors. For example, future studies may examine the water content in the control and stimulated tissues of the young and mature internodes and identify constituents that are responsible for the viscous characteristics of the tissue.